2005-12

Hyperspectral imaging using ultraviolet light

Porter, Michael A.

Monterey, California. Naval Postgraduate School

NAVAL POSTGRADUATE SCHOOL

MONTEREY, CALIFORNIA

THESIS

HYPERSPECTRAL IMAGING USING ULTRAVIOLET LIGHT

by

Michael Anthony Porter

December 2005

Thesis Advisor:	Richard C. Olsen
Co-Advisor:	Christopher Brophy

Approved for public release; distribution is unlimited

THIS PAGE INTENTIONALLY LEFT BLANK

REPORT DOCUMENTATION PAGE			Form Approved OMB No. 0704-0188
Public reporting burden for this collection of information is estimated to average 1 hour per response, including the time for reviewing instruction, searching existing data sources, gathering and maintaining the data needed, and completing and reviewing the collection of information. Send comments regarding this burden estimate or any other aspect of this collection of information, including suggestions for reducing this burden, to Washington headquarters Services, Directorate for Information Operations and Reports, 1215 Jefferson Davis Highway, Suite 1204, Arlington, VA 22202-4302, and to the Office of Management and Budget, Paperwork Reduction Project (0704-0188) Washington DC 20503.			
1. AGENCY USE ONLY ***(Leave blank)***	**2. REPORT DATE** December 2005	**3. REPORT TYPE AND DATES COVERED** Master's Thesis	
4. TITLE AND SUBTITLE: Title (Mix case letters) Hyperspectral Imaging Using Ultraviolet Light			**5. FUNDING NUMBERS**
6. AUTHOR(S)			
7. PERFORMING ORGANIZATION NAME(S) AND ADDRESS(ES) Naval Postgraduate School Monterey, CA 93943-5000			**8. PERFORMING ORGANIZATION REPORT NUMBER**
9. SPONSORING /MONITORING AGENCY NAME(S) AND ADDRESS(ES) N/A			**10. SPONSORING/MONITORING AGENCY REPORT NUMBER**
11. SUPPLEMENTARY NOTES The views expressed in this thesis are those of the author and do not reflect the official policy or position of the Department of Defense or the U.S. Government.			
12a. DISTRIBUTION / AVAILABILITY STATEMENT Approved for public release; distribution is unlimited			**12b. DISTRIBUTION CODE**

13. ABSTRACT (maximum 200 words)

The LINEATE IMAGING NEAR ULTRAVIOLET SPECTROMETER (LINUS) instrument has been used to remotely detect and measure sulfur dioxide (SO_2). The sensor was calibrated in the lab, with curves of growth created for the $0.29 - 0.31\mu$ spectral range of the LINUS sensor. Field observations were made of a coal burning plant in St. John's, Arizona at a range of 537 m. The Salt River Coronado plant stacks were emitting on average about 100 ppm and 200 ppm from the left and right stacks respectively. Analysis of the LINUS data matched those values within a few percent. Possible uses for this technology include remote verification of industry emissions and detection of unreported SO_2 sources.

14. SUBJECT TERMS Sulfur Dioxide (SO_2), Remote Sensing, Ultraviolet (UV) Spectral Imaging, LINUS			**15. NUMBER OF PAGES** 73
			16. PRICE CODE
17. SECURITY CLASSIFICATION OF REPORT Unclassified	**18. SECURITY CLASSIFICATION OF THIS PAGE** Unclassified	**19. SECURITY CLASSIFICATION OF ABSTRACT** Unclassified	**20. LIMITATION OF ABSTRACT** UL

NSN 7540-01-280-5500 Standard Form 298 (Rev. 2-89)
Prescribed by ANSI Std. 239-18

THIS PAGE INTENTIONALLY LEFT BLANK

Approved for public release; distribution is unlimited

HYPERSPECTRAL IMAGING USING ULTRAVIOLET LIGHT

Michael A. Porter
Lieutenant Commander, United States Navy
B.A. and B.S., Southeast Missouri State University, 1990
M.N.S., Southeast Missouri State University, 1992

Submitted in partial fulfillment of the
requirements for the degree of

MASTER OF SCIENCE IN ASTRONAUTICAL ENGINEERING

from the

NAVAL POSTGRADUATE SCHOOL
December 2005

Author: Michael A. Porter

Approved by: Dr. Richard C. Olsen
Thesis Advisor

Dr. Christopher Brophy
Co-Advisor

Dr. Anthony J. Healey
Chairman, Department of Mechanical and Astronautical Engineering

THIS PAGE INTENTIONALLY LEFT BLANK

ABSTRACT

The LINEATE IMAGING NEAR ULTRAVIOLET SPECTROMETER (LINUS) instrument has been used to remotely detect and measure sulfur dioxide (SO_2). The sensor was calibrated in the lab, with curves of growth created for the $0.29-0.31\mu$ spectral range of the LINUS sensor. Field observations were made of a coal burning plant in St. John's, Arizona at a range of 537 m. The Salt River Coronado plant stacks were emitting on average about 100 ppm and 200 ppm from the left and right stacks respectively. Analysis of the LINUS data matched those values within a few percent. Possible uses for this technology include remote verification of industry emissions and detection of unreported SO_2 sources.

THIS PAGE INTENTIONALLY LEFT BLANK

TABLE OF CONTENTS

THIS PAGE INTENTIONALLY LEFT BLANK

LIST OF FIGURES

LIST OF TABLES

THIS PAGE INTENTIONALLY LEFT BLANK

ACKNOWLEDGMENTS

My love and appreciation to my wife Judi for putting up with the long hours I spent at school while she entertained three small children at home. My love and thanks to Sarah, David, and Michelle for always welcoming me home with happy enthusiasm!

Many thanks to Dr. Richard C. Olsen for taking me on as a thesis student and his guidance during all aspects of this work.

Thanks to Dr. Christopher Brophy for his guidance and agreeing to be my co-advisor.

Dr. D. Scott Davis was instrumental in guiding me concerning curves of growth.

Richard and Lynda Harkins worked very hard as we collected the data in Arizona and endured the long road trip.

Angie Puetz also endured the long road trip. Thank you Angie for teaching me IDL, helping me with ENVI, and the data analysis you did!

Sing Soong Khoo first showed me how to operate LINUS and I used much of his data in this thesis.

Thanks to Mr. James Wood, Mr. Lee Murdock, Mr. Chris Janick, Mr. Jerry Bicknell, and the entire Salt River Project Coronado plant workforce. This work could not have been done successfully without their kind assistance.

THIS PAGE INTENTIONALLY LEFT BLANK

I. INTRODUCTION

A. OBJECTIVE OF RESEARCH

The detection and quantification of gases in the atmosphere is an important task in both civil and military/intelligence areas. A relatively common gas of interest is Sulfur Dioxide (SO_2). Sulfur Dioxide is of interest to volcanologists[1] and is of great interest in the context of industrial facilities particularly coal-fired power plants.[2] SO_2 can be measured in a variety of spectral ranges, including ultraviolet (UV)[3] and long-wave infrared (LWIR)[4]. Previous work in the UV has focused on the use of point measurements of plumes. There is a need for broader measurements, with instruments combining spectral and imaging characteristics.

The objective of this thesis is the remote detection of gases using the Lineate Imaging Near Ultraviolet Spectrometer (LINUS). Several theses have been completed covering the physical construction, calibration, software, and interface for LINUS. This thesis will present the first field work to yield corroborated measurements of an industrial SO_2 source.

LINUS is the third generation of imaging spectrometers built at the Naval Postgraduate School. LINUS is an improvement in that it is useful over a broader range of wavelengths (with appropriate filters), is more sensitive, and has greater spectral resolution.

B. SPECTRAL IMAGING

Spectral chemical analysis is the study of the interactions and relationship between atoms and molecules and electromagnetic radiation. The electromagnetic spectrum is shown in Figure 1 and extends from the infrared to gamma rays. The speed of light in a vacuum, c, is nearly $3x10^8 m/s$ and can be related to frequency, ν, and

[1] USGS website.

[2] EPA website.

[3] USGS website.

[4] Mares.

wavelength, λ, by the relationship $c = \lambda\nu$. In terms of energy, the shorter the wavelength (hence the higher the frequency) of the radiation, the higher the energy of the photon.

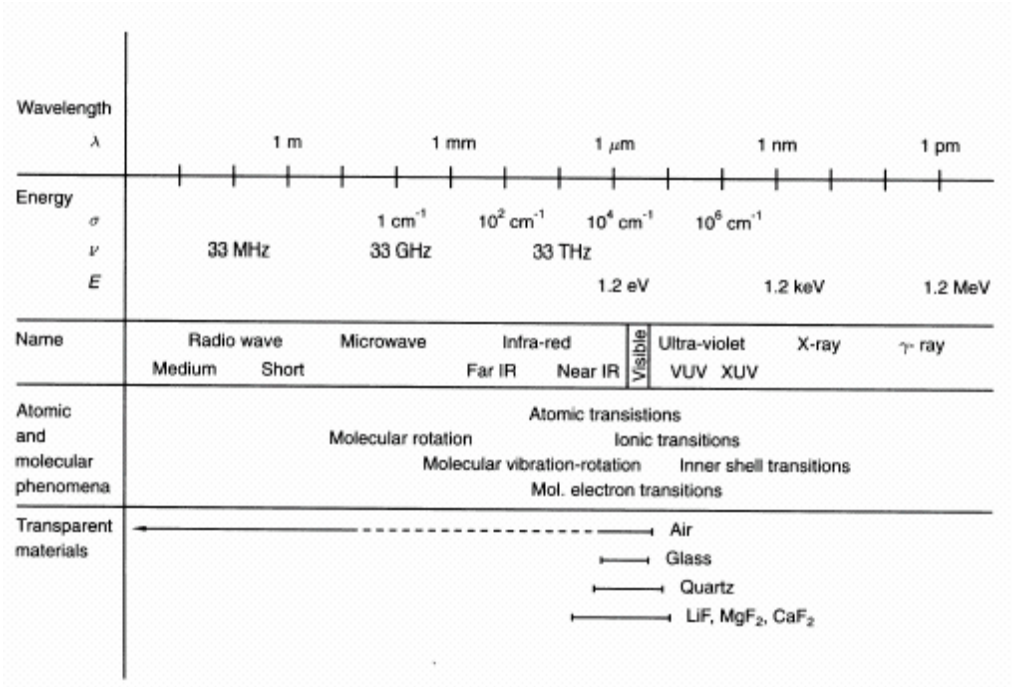

Figure 1 The electromagnetic spectrum (from Thorne et al., 1999)

It was discovered in the early 20th century that energy is quantized and that $E = h\nu$ where E is energy in Joules, h is Plank's constant ($6.62607x10^{-34} J\cdot s$), and ν is frequency in Hertz (s^{-1}). A photon can be characterized by wavelength, frequency, wave number (σ), or energy. The literature widely uses wave number where $\sigma = \frac{1}{\lambda_{vacuum}}$ and is most commonly expressed in cm^{-1}. This is not an SI unit but is very widely used instead of m^{-1}. Since LINUS measures the intensity of UV light versus wavelength, this thesis uses wavelength. The various nomenclatures are illustrated in Figure 1.

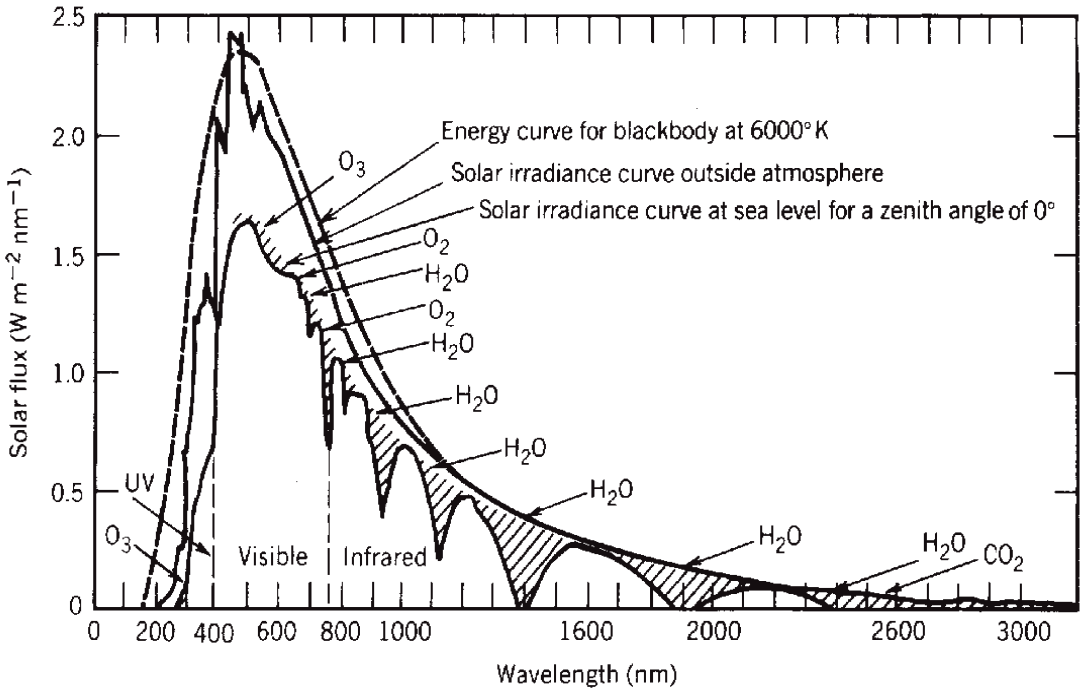

Figure 2 6000 K blackbody radiation curve superimposed over solar irradiance curves above and below the atmosphere (from Finlayson-Pitts & Pitts, 1986)

$$\overline{D} = \varepsilon \overline{E}$$
$$\mu \overline{H} = \overline{B}$$
$$\overline{J} = \gamma \overline{E}$$
$$\nabla \times \overline{E} = -\frac{\delta \overline{B}}{\delta t}$$
$$\nabla \times \overline{H} = \overline{J} + \frac{\delta \overline{D}}{\delta t}$$
$$\nabla \cdot \overline{B} = 0$$
$$\nabla \cdot \overline{D} = \rho$$

Figure 3 Maxwell's Equations which describe the behavior of electromagnetic waves. D is electric flux density, E is electric field strength, ε is dialectric constant, μ is permeability, H is magnetic intensity, B is magnetic flux density, J is current density, γ is conductivity, and ρ is density of electric charge.

Electromagnetic radiation is absorbed and emitted by atoms and molecules. When a molecule absorbs a photon this causes a valence electron to jump to a higher energy state. The study of fine spectral structures can reveal much about a molecule.

This same study extended to the gamma ray region can reveal much about the nuclear structure of atoms. This thesis makes use of the larger scale features of molecular absorption (electronic transitions) and does not exploit the rotational and vibrational energy state transitions. LINUS is designed to detect the absorption of ambient UV from the sun caused by the presence of SO_2. Figure 4 illustrates the effect of wavelength on the absorptivity of SO_2.

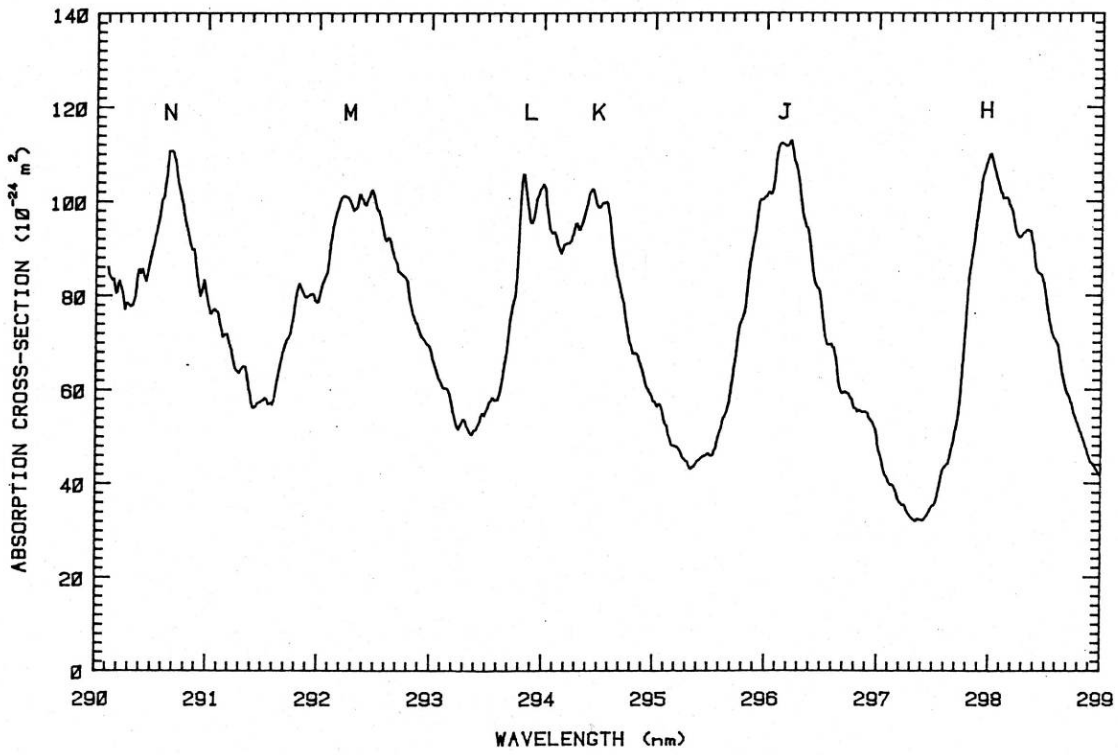

Figure 4 Variation of absorption cross section of SO_2 with wavelength (from Brassington, 1981)

C. SULFUR DIOXIDE

Sulfur Dioxide is a naturally occurring gas in the atmosphere. The major constituents of the atmosphere are seen in Table 1.

Constituent Name / (type)	Formula	Molecular Mass	% by volume
Nitrogen/ (Permanent)	N_2	28.0134	78.084
Oxygen / (Permanent)	O_2	31.9988	20.9476
Argon / (Permanent)	Ar	39.948	0.934
Water Vapor / (Variable)	H_2O	18.0160	0-7
Carbon Dioxide / (Variable)	CO_2	44.00995	0.01-0.1
Ozone / (Variable)	O_3	47.9982	0-0.01
Neon / (Permanent)	Ne	20.183	0.001818
Helium / (Permanent)	He	4.0026	0.000524
Methane / (Permanent)	CH_4	16.04303	0.0002
Sulfur Dioxide / (Variable)	SO_2	64.064	0-0.0001
Hydrogen / (Permanent)	H_2	2.01594	0.00005
Nitrogen Dioxide / (Variable)	NO_2	46.0055	0-0.000002

Table 1. Atmospheric constituents by volume % (from Durkee, 1999)

SO_2 is formed by the combination of Sulfur and Oxygen,

$$S + O_2 = SO_2 \tag{1.1}$$

and is considered to be "probably the most significant single air pollutant."[5] SO_2 is released naturally into the atmosphere by volcanoes which are by far the largest source.[6] Manmade sources are tied to the burning of fuels which contain sulfur such as petroleum and coal. Burning fuels with lower sulfur content reduces the production of SO_2. SO_2 is considered to be a problem because of its impact upon human health and the environment. SO_2 readily combines with water vapor to form sulfuric acid which then falls to the earth in rain or snow. This "acid rain" damages natural waterways and accelerates the corrosion of manmade structures.[7]

Efforts to reduce SO_2 production focus on reducing industrial emissions. In the United States, industries are allotted a certain SO_2 emission allowance and must buy the right to emit more than that allowance. This has resulted in a thriving trade in SO_2 allowances. The following from the EPA website gives some insight:

[5] Southern Technologies, Inc. website.

[6] Halvatzis.

[7] EPA website.

An allowance authorizes a unit within a utility or industrial source to emit one ton of SO_2 during a given year or any year thereafter. At the end of each year the unit must hold an amount of allowances at least equal to its annual emissions, i.e., a unit that emits 5,000 tons of SO_2 must hold at least 5,000 allowances that are usable in that year. However, regardless of how many allowances a unit holds, it is never entitled to exceed the limits set under Title I of the Act to protect public health.

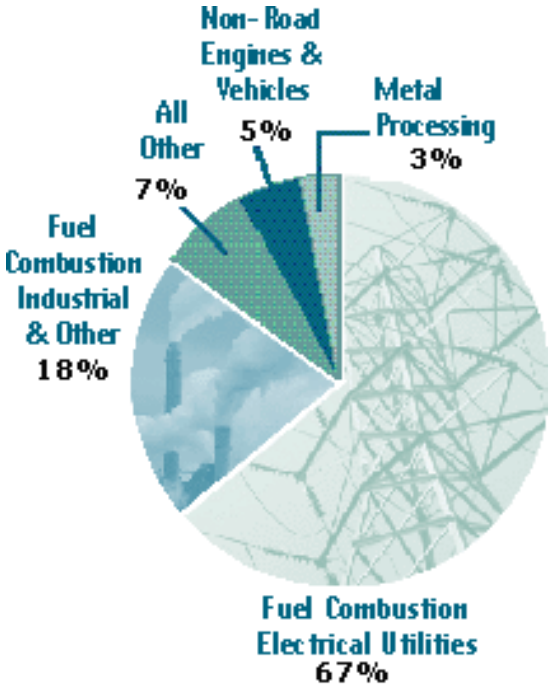

Figure 5 Man made sources of SO_2 (from EPA website)

Allowances are fully marketable commodities. Once allocated, allowances may be bought, sold, traded, or banked for use in future years. Allowances may not be used for compliance prior to the calendar year for which they are allocated.

Allowances are allocated for each year beginning in 1995. Phase I included certain electricity generating units. EPA allocated allowances at an emission rate of 2.5 pounds of SO_2/mmBtu (million British thermal units) of heat input (3.88 kg SO_2/MW-Hr), multiplied by the unit's baseline mmBtu (the average fossil fuel consumed from 1985 through 1987). These allowance allocations are listed in Table A of the Clean Air Act and codified in the Allowance System Regulations (Part 73, Table 1). Alternative or additional allowance allocations were made for various units, including affected units in Illinois, Indiana, and Ohio, which were allocated a pro rata share of 200,000 additional allowances each year from 1995 to 1999.

In Phase II, which began in the year 2000, EPA expanded the group of affected sources to include virtually all units over 25 MW in generating capacity, and tightened the allowance allocation. Allowance allocation calculations were made for various types of units, such as coal- and gas-fired units with low and high emissions rates or low fuel consumption. EPA allocated allowances to each unit at an emission rate of 1.2 pounds of SO_2/mmBtu of heat input, multiplied by the unit's baseline. During Phase II, the Act places a cap at 8.95 million on the number of allowances issued to units each year. This effectively caps emissions at 8.95 million tons annually and ensures that the mandated emissions reductions are maintained over time.[8] (Note that $1\ \text{ton} \equiv 907.18$ kg and $1x10^6 BTU \equiv 0.2928751 MW \square Hr$).

[8] EPA website.

SO_2 causes a wide variety of health and environmental impacts because of the way it reacts with other substances in the air. Particularly sensitive groups include people with asthma who are active outdoors and children, the elderly, and people with heart or lung disease.

Respiratory Effects from Gaseous SO_2
Peak levels of SO_2 in the air can cause temporary breathing difficulty for people with asthma who are active outdoors. Longer-term exposures to high levels of SO_2 gas and particles cause respiratory illness and aggravate existing heart disease.

Respiratory Effects from Sulfate Particles
SO_2 reacts with other chemicals in the air to form tiny sulfate particles. When these are breathed, they gather in the lungs and are associated with increased respiratory symptoms and disease, difficulty in breathing, and premature death.

Visibility Impairment
Haze occurs when light is scattered or absorbed by particles and gases in the air. Sulfate particles are the major cause of reduced visibility in many parts of the U.S., including our national parks.

Acid Rain
SO_2 and nitrogen oxides react with other substances in the air to form acids, which fall to earth as rain, fog, snow, or dry particles. Some may be carried by the wind for hundreds of miles.

Plant and Water Damage
Acid rain damages forests and crops, changes the makeup of soil, and makes lakes and streams acidic and unsuitable for fish. Continued exposure over a long time changes the natural variety of plants and animals in an ecosystem.

Aesthetic Damage
SO_2 accelerates the decay of building materials and paints, including irreplaceable monuments, statues, and sculptures that are part of our nation's cultural heritage.

Figure 6 Negative aspects of atmospheric SO_2 (from the EPA website)

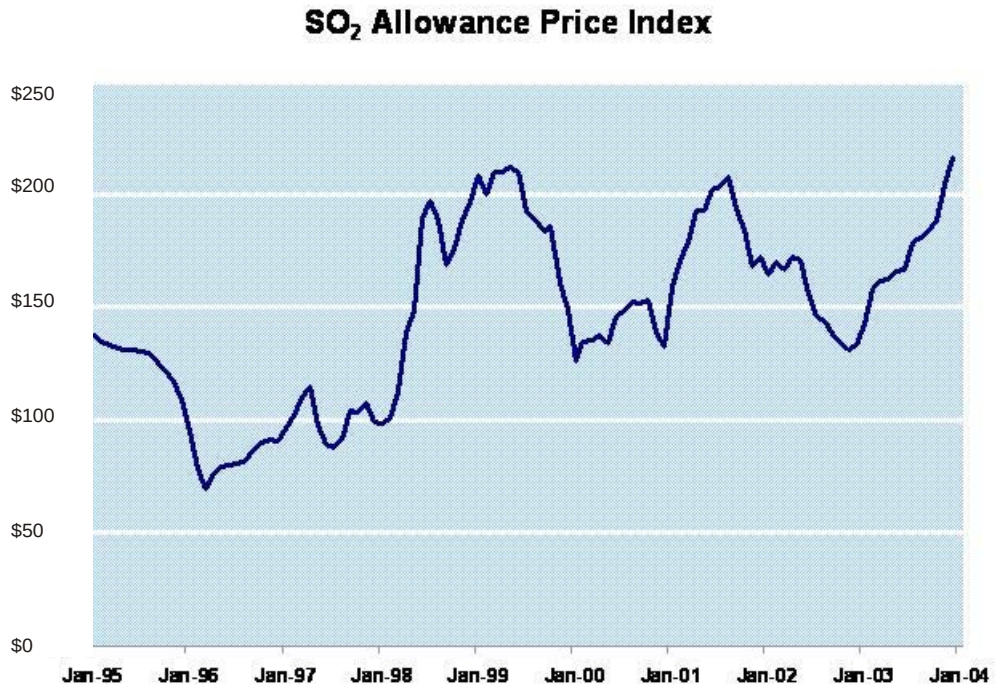

Figure 7 SO_2 Allowance prices as reported by the EPA

Since power plants can sell their allowances, it is in their best interest to reduce their own emissions. The allowances that are not used can be sold for a profit.

SO_2 is such an important component of the atmosphere, both from an environmental and economic viewpoint, that it was deemed to be a good gas to attempt to detect.

D. PREVIOUS WORK

Several theses have been written at the Naval Postgraduate School concerning detection of SO_2. In 1999 Marino[9] conducted field work using the Naval Postgraduate School's Ultraviolet Imaging Spectrometer (NUVIS) which was the forerunner to LINUS. Marino conducted work very similar to the present work and did detect SO_2.

[9] Marino.

Halvatzis[10] was the first to report results from the field using LINUS. He used LINUS to image sulfuric plumes at Lassen Volcanic National Park. He was successful in detecting SO_2 but had problems with quantification due to difficulty in finding an SO_2-free Blue Sky background reference. Khoo[11] was the first to use LINUS to image industrial emissions. He imaged an oil refinery in Concord, California. SO_2 was detected but there were image saturation problems which precluded quantification.

In addition to research at the Naval Postgraduate School, recent work has been done using very small spectrometers built by Ocean Optics Inc. In January 2004 these spectrometers were used in conjunction with laptop computers to calculate the volcanic plume velocity at Masaya volcano, Nicaragua.[12]

[10] Halvatzis.

[11] Khoo.

[12] McGonigle, et al.

II. BACKGROUND

A. DESCRIPTION OF LINUS

LINUS (Lineate Near Ultraviolet Spectrometer) was designed and built at the Naval Postgraduate School by Dr. D. Scott Davis. Several theses have been completed on lab work related to the construction and calibration of the instrument. The last major hardware change was the addition of a visual camera by Rodrigo Cabezas in 2002. The visual camera made it possible to "see" bore-sighted what LINUS is pointed at instead of guessing. In addition to adding the camera Cabezas modified the control software in order to take advantage of the new hardware. A brief review of this previous work is given here. For a more detailed description see Cabezas and Gray.

The schematic layout of LINUS is presented in Figure 8, the optical layout of LINUS is presented in Figure 9, and photographs of the interior and exterior in Figure 10 and Figure 11. Photons from the target pass through the aperture and reflect off of the scanning mirror. The rays then pass through the UV filter and primary objective lens, through the slit assembly, and then through the collimating lens. The rays then reflect off of the reflecting grating which breaks the spectrum into distinct wavelengths, pass through the camera objective lens, and are measured by the Princeton UV intensified camera.

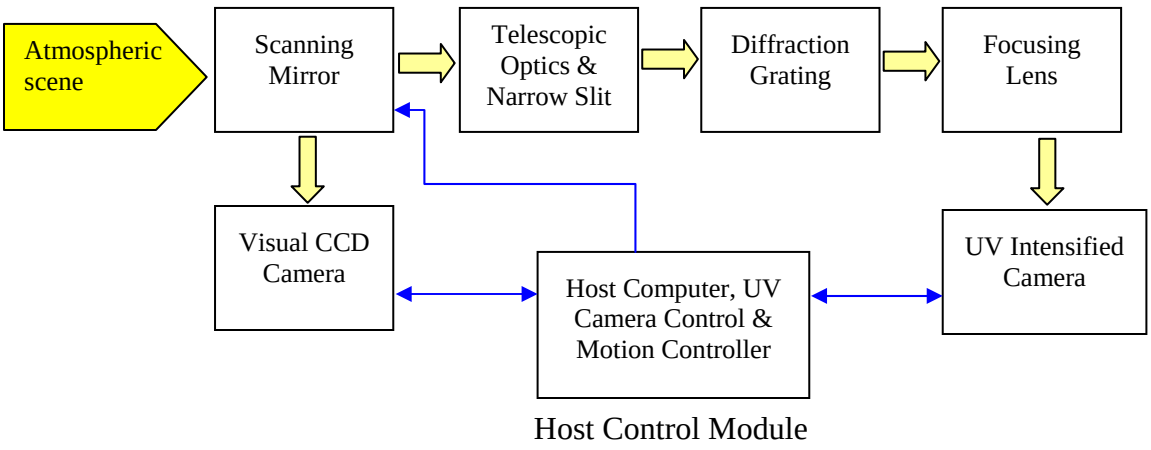

Figure 8 Schematic Block Diagram for LINUS (from Khoo)

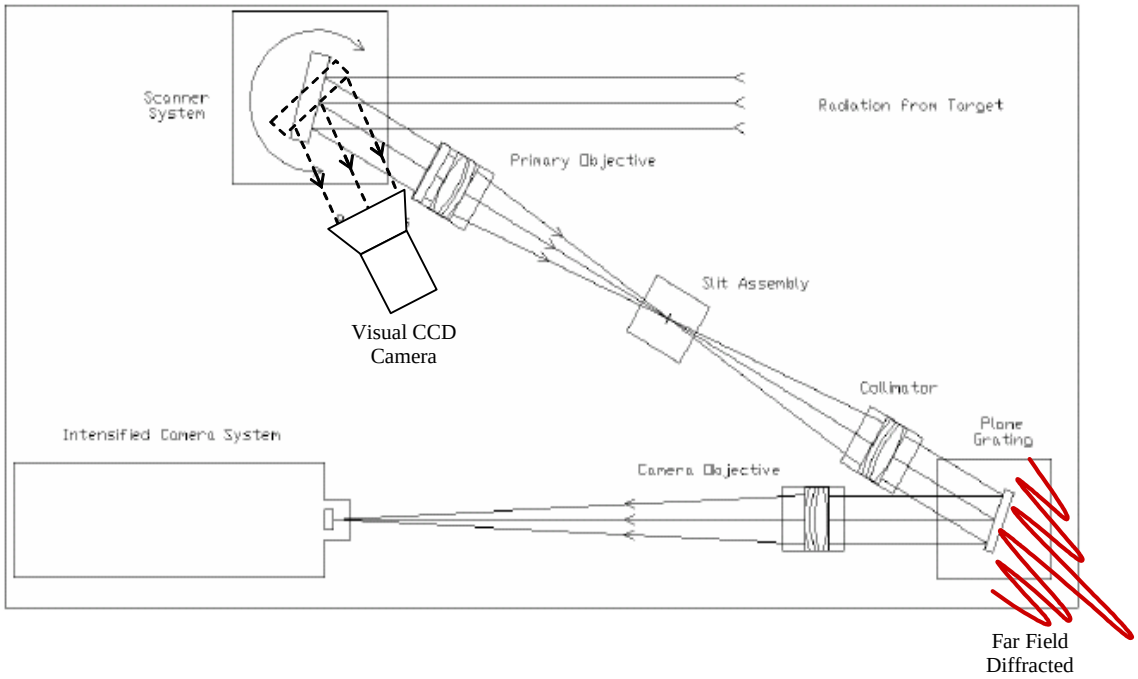

Figure 9 Optical Layout of LINUS (from Davis)

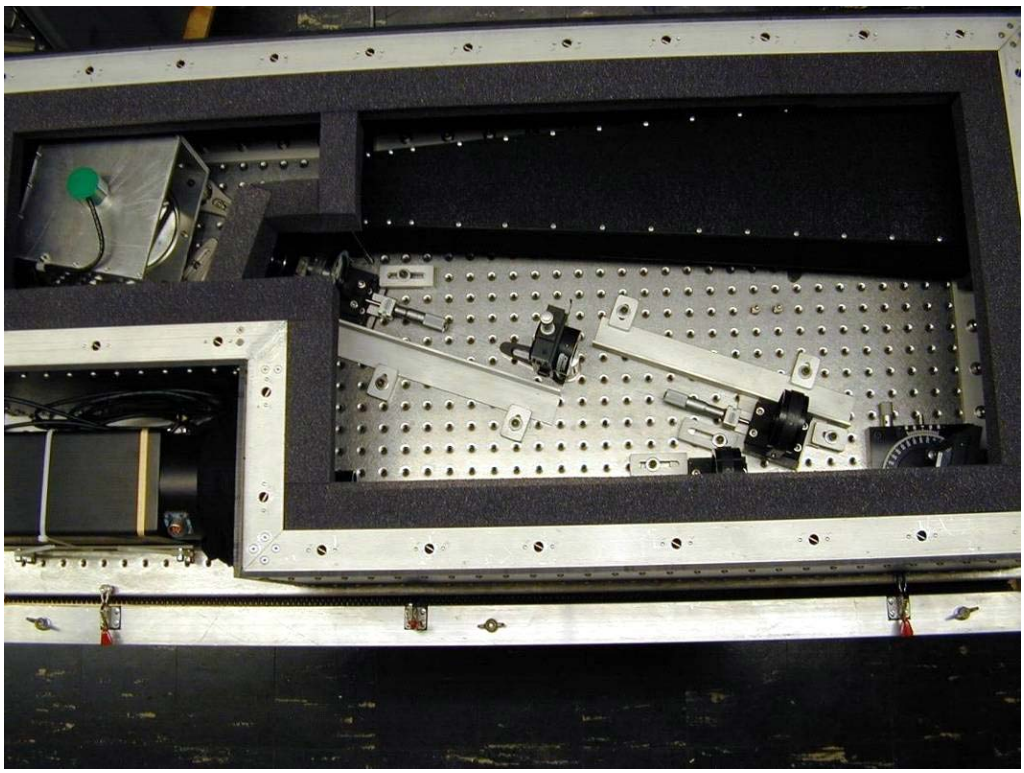

Figure 10 Interior View of LINUS (from Gray)

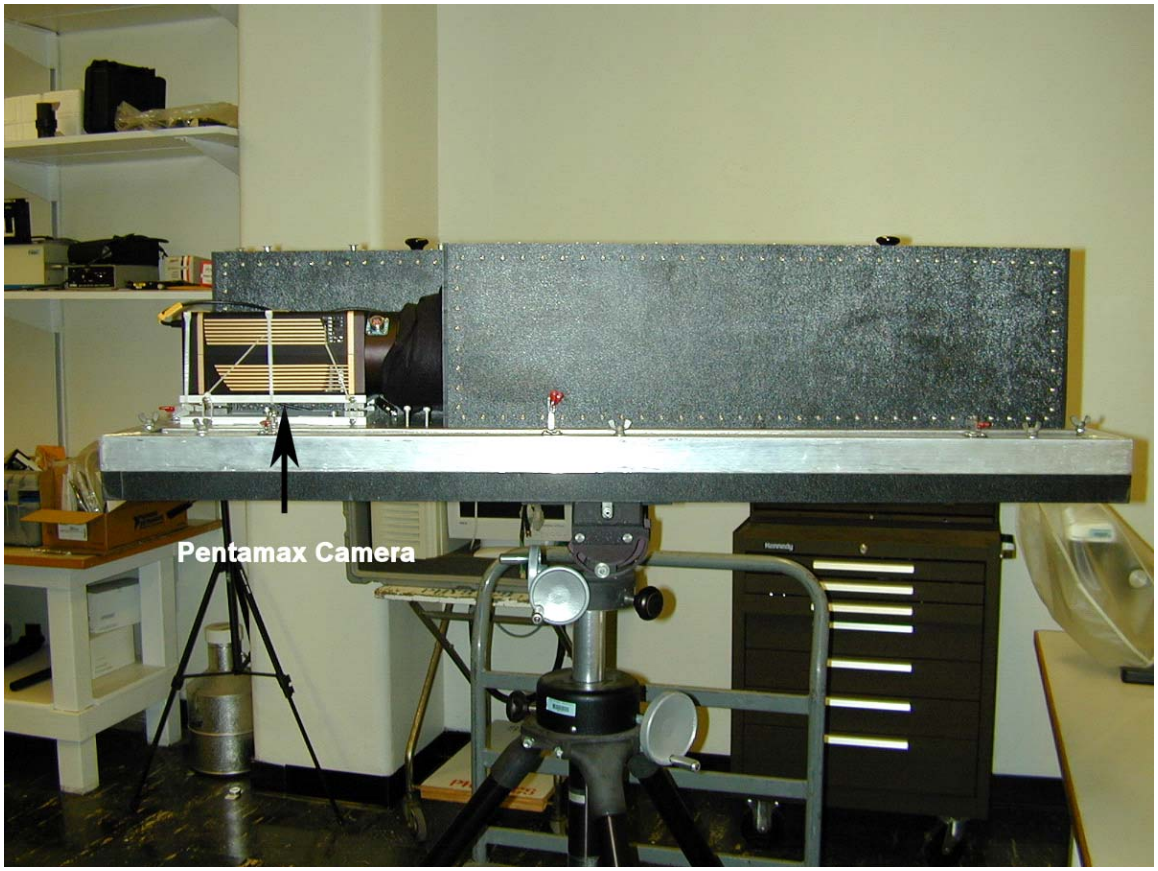

Figure 11 Side view of LINUS (from Gray)

The optical system is mounted to a standard optical bench with dimensions 58.5 cm wide by 119 cm long by 23.2 cm deep. The entire assembly is encased in black Acrylonitryl Butadien Styrene which is coated on the interior with black felt. The cover is removable using quick release Dzus fasteners.[13] The cover is normally removed only for set up, take down, and when it is desired to adjust the slit width.

The UV filter used in LINUS has band pass characteristics as seen in Figure 12. Maximum response is just below 300 nm. Note that the UV transmission drops rapidly above and below 300 nm, hence there is very little system response outside of the 290-310 nm range. Under very low UV conditions it is possible to

[13] Gray.

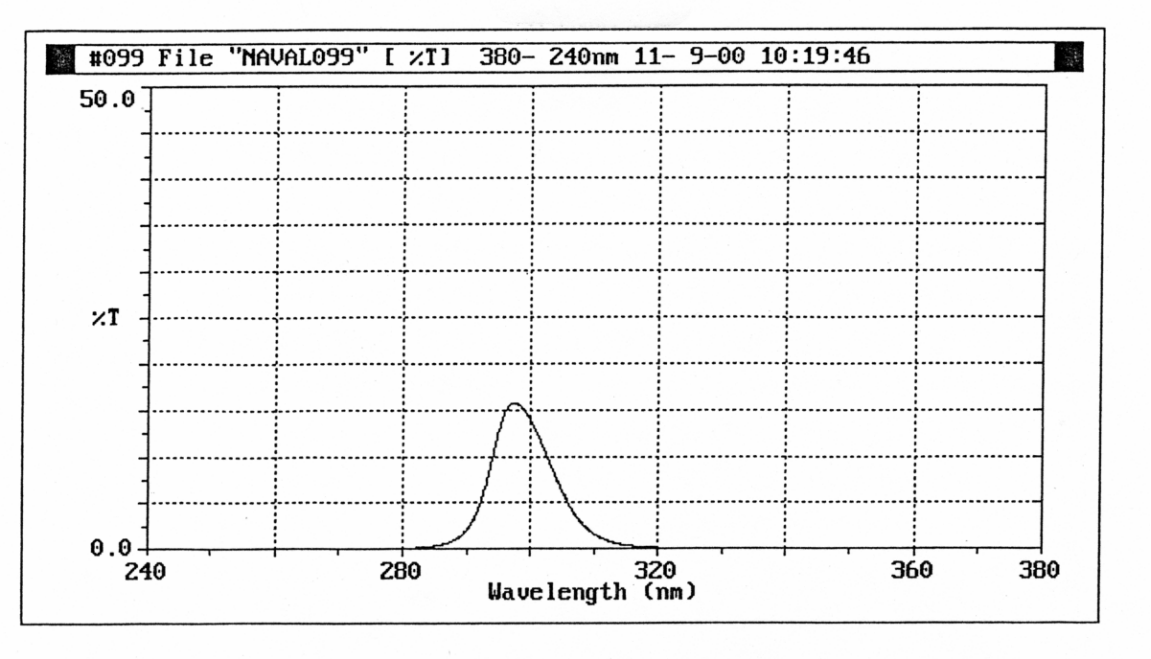

Figure 12 Filter Response Function (from Gray)

allow more UV into the camera by making the slit width larger. This allows a wider horizontal FOV, allowing more light energy to reach the camera CCD. The downside to this is less spatial resolution. According to Thorne[14] the optimum slit width is on the order of $10\mu m$ and often is a little wider.

Wavelength calibration was completed in 2003 by Cabezas using a Platinum lamp. This allowed an accurate correlation between pixel and wavelength, yielding the equation $\lambda = 277.658 + .08299 \bullet column$.[15]

The diffraction grating used in LINUS is 2 cm x 2 cm and is ruled with 600 lines per millimeter which is a standard ruling. Figure 13 illustrates the function of the diffraction grating in LINUS.

[14] Thorne, et al.

[15] Cabezas.

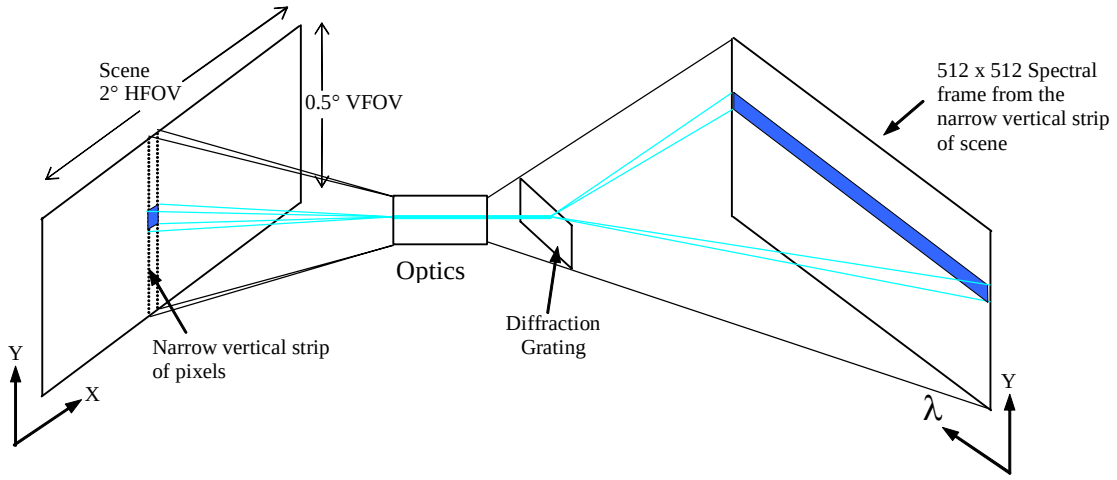

Figure 13 Depiction of light path through LINUS (from Khoo)

The scanning mirror is controlled by a stepping motor which has a resolution of 144,000 counts per revolution.[16] The stepping motor is controlled by a Labview software (a product of National Instruments Corporation) interface which was designed and incorporated by Cabezas.

The camera used is the Princeton Instruments Intensified PentaMAX. The camera utilizes a Micro Channel Plate (MCP) which is coupled to the 512 x 512 pixel charge-coupling device (CCD) array.[17] Voltage to the MCP is adjustable to vary the gain.

The instrument is pointed at the object (such as a smokestack) to acquire an image. The desired exposure time for each step, the number of stepping motor counts per step, and the total number of steps is entered. Exposure time varies with the ambient UV intensity and may need to be adjusted throughout the day. If adjusted it is imperative that a new Blue Sky image be acquired as a reference. Figure 14 shows the Labview screen where the inputs are made.

[16] Halvatzis.

[17] Gray.

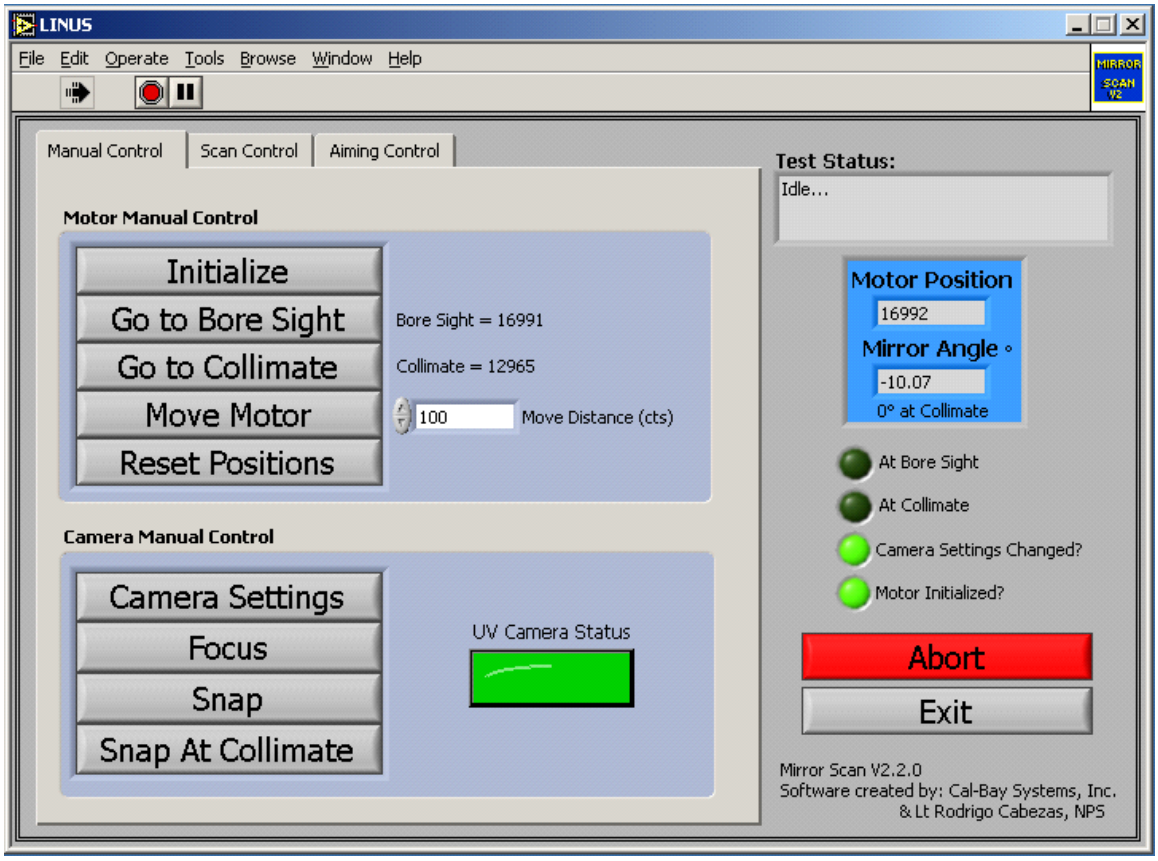

Figure 14 Labview LINUS interface screen (from Khoo)

After all of the inputs are made, image acquisition is begun and the stepping motor will move the scanning mirror in between scenes. The individual scenes can overlap, be exactly coincident (step size equals zero), or not overlap at all depending on what is desired. These individual scenes are illustrated in Figure 16. The maximum horizontal FOV is 2°.[18]

Figure 15 is a view of the smokestacks as seen through the visual camera installed by Cabezas. This picture has been reversed to remove the effect of the mirror.

[18] Halvatzis.

Figure 15 Smokestacks as seen through LINUS's visual camera.

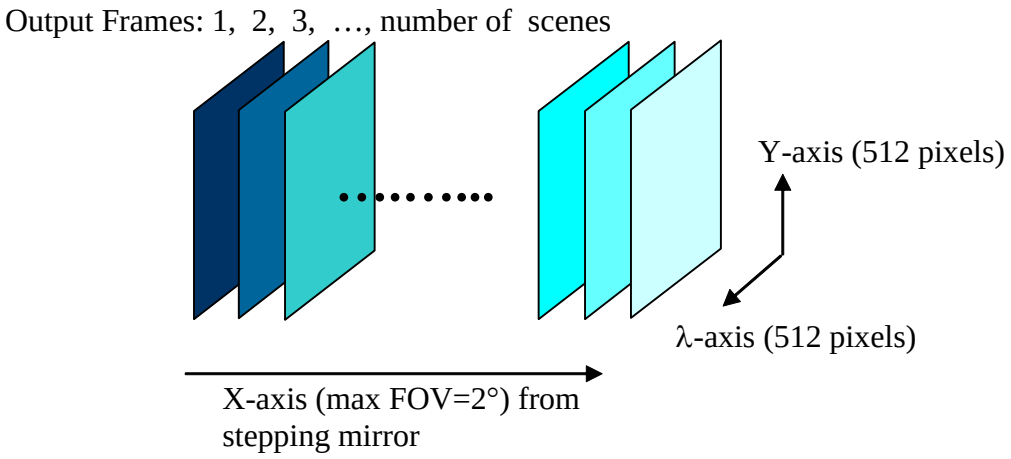

Figure 16 Hyper Spectral Data Cube Formed by LINUS Output (from Khoo)

Each frame then images an area 0.5° high (vertical field of view) and a variable width (0.023° wide with a slit width of 0.1 mm). The horizontal instantaneous FOV (IFOV) is varied by adjusting the slit width. From Halvatzis[19] we have Equation (2.1),

$$\theta_{horiz} = 2 \times \tan^{-1}\left(\frac{w}{2 \times f}\right) \tag{2.1}$$

Here w is the slit width and f = 25cm which is the focal length of the primary objective lens. For example, if the slit width is 0.1 mm the IFOV $\theta_{horiz} = 0.023^{\circ}$. For the Arizona trip the camera was 537 m from the plume and the slit width was 0.1 mm so each instantaneous snapshot had an IFOV that was 21.5 cm wide and 4.7 m vertical. The vertical image is 512 pixels high and the horizontal image is 512 pixels wide. Due to the action of the diffraction grating, the intensity recorded on each pixel is the intensity of a specific wavelength. So LINUS records vertical and wavelength data with each step. The third dimension, horizontal spatial, is made possible by the action of the stepping motor. The stepping motor rotates the scanning mirror between each scene the specified number of steps.

[19] Halvatzis.

III. DESCRIPTION OF DATA COLLECTION

A. PURPOSE

LINUS has been operated a number of times in the field, but good data with "ground truth" confirmation have been sorely lacking. These previous experiments included two trips by Khoo to a refinery in Concord, California. In order to collect data that would support quantification it was deemed prudent to look outside California for a coal burning power plant. The coal burning power plant owned by the Salt River Project in St. Johns, Arizona turned out to be a perfect place to collect data.

B. PLANT OVERVIEW

The Salt River Project Coronado power generating plant in St. Johns sits at 34°34.5' North latitude and 109°16.63' West longitude. The altitude is 1810 m. The plant has a maximum capacity of 785 MW including one 395 MW unit and one 390 MW unit. The plant burns a maximum of 9,135 tons of coal per day at maximum power. The coal is brought in by rail from Wyoming and has a 0.5% Sulfur content. Electrostatic precipitators are used in the exhaust system to control fly ash and scrubbers are used to remove SO_2. This information is summarized in Figure 17.

> SRP is two entities: the Salt River Project Agricultural Improvement and Power District, a political subdivision of the state of Arizona; and the Salt River Valley Water Users' Association, a private corporation.
>
> The District provides electricity to nearly 860,000 retail customers in the Phoenix area. It operates or participates in 11 major power plants and numerous other generating stations, including thermal, nuclear, natural gas and hydroelectric sources. [20]

[20] Salt River Project homepage.

Coronado Generating Station

Owner/Operator: Owned and operated by Salt River Project (SRP).

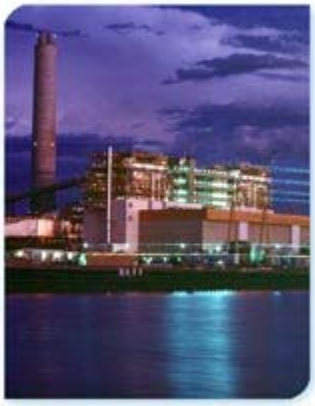

Description: Coal-fired, steam electric generating station.

Capacity: 785 megawatts, from one 395 MW unit and one 390 MW unit.

Fuel source: Coal. The sulfur content of the coal is 0.5 percent.

Coal consumption: A maximum of 9,135 tons per day if both units are running at full load.

Plant construction: Construction began 1975. Unit 1 completed Dec. 31, 1979. Unit 2 completed Oct. 1, 1980.

Construction costs: $700 million, including $220 million in environmental control equipment.

Environmental control equipment:

- Electrostatic precipitators to control fly ash.
- Scrubbers to remove sulfur dioxide (SO_2).
- Water reservoir is lined to help recover and contain process waste.

Figure 17 Salt River Project Coronado Generating Station

C. DATA GATHERING TRIP

A great deal of experience had been gleaned from Khoo's data gathering trips. LINUS is quite bulky and it takes a minimum of two strong individuals to set up the camera. The field team consisted of four people: Mr. Richard Harkins, Mrs. Lynda Harkins, Ms. Angela Puetz, and the author. Prior to departure from Monterey a briefing

was conducted to ensure that no important details had been forgotten and that everyone understood the plan. The pre-deployment checklist is included in the appendices.

Due to the distance to St. Johns an entire week was allotted for the trip. The team departed Monterey at 0800 Monday April 11, 2005. Two vehicles were necessary to transport all of the personnel and equipment, a rental minivan and Mr. Harkins' truck. The first night of the trip was spent in Kingman, Arizona with arrival in St. Johns the afternoon of April 12.

Upon arrival at the plant the whole team had to first have a security and safety in brief. Several videos were viewed explaining the safety and security procedures. Everyone was issued a hardhat, safety goggles, and a security badge.

It was decided that the best place to set up the equipment was the parking lot near the credit union outside the security fence. This spot offered a clear view of the smokestack as well as safe and convenient access.

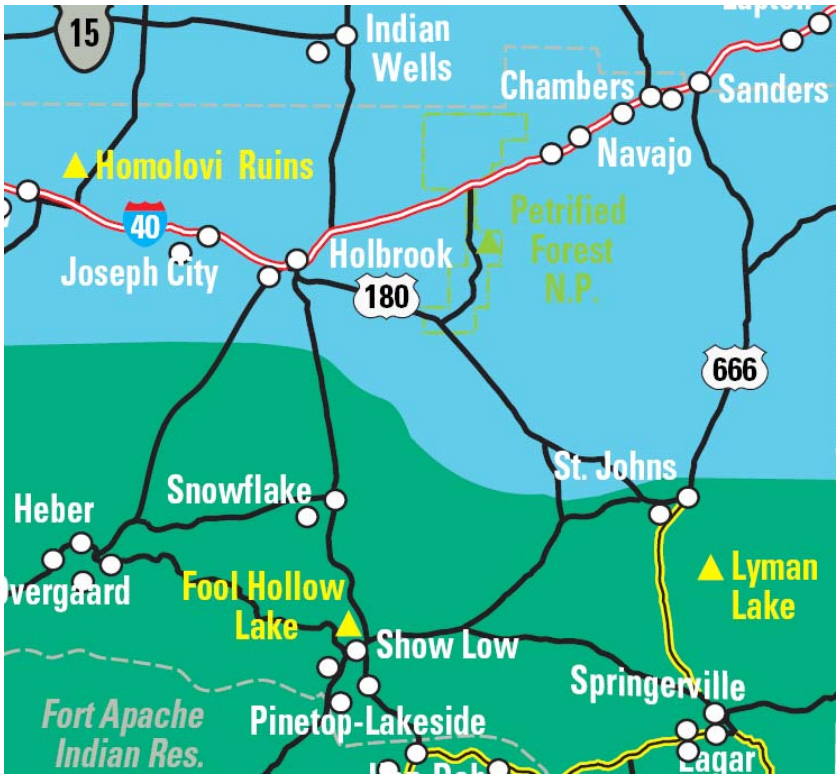

Figure 18 St. Johns, Arizona and surrounding area (from State of Arizona website)

A small patio tent was set up to protect the equipment from overheating and to give personnel some protection. At these high altitudes the UV is fairly strong.

Figure 19 Left to right, Lynda Harkins, Richard Harkins, Angela Puetz, and the author

Data collection commenced on April 13 and continued on April 14 and 15. The weather was fairly consistent all three days with clear skies and some high cirrus clouds in the afternoon. Temperatures ranged from 18C in the mornings to 24C in the mid afternoon. Humidity stayed at about 10% with atmospheric pressure at about 617 Torr. Wind speed varied from 0 m/s in the morning up to 2 m/s at mid-day.

Figure 20 Richard Harkins collecting LINUS data

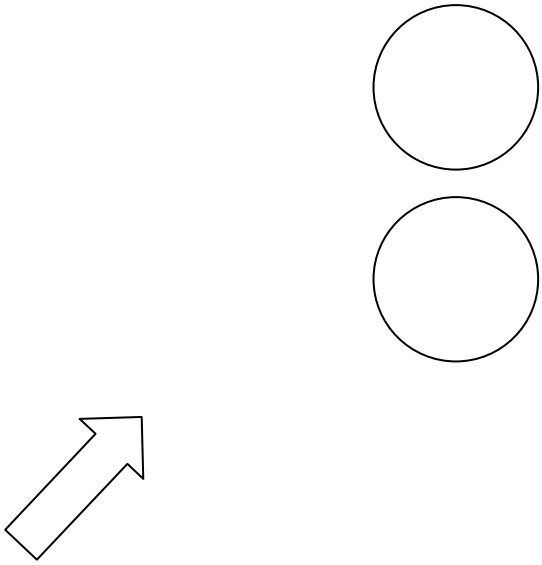

Figure 21 Collection Geometry showing smoke stacks and viewing direction

Figure 22 View of LINUS pointing at the smoke stacks

IV. ANALYSIS

A. PURPOSE

Having taken data at Salt River Project Coronado power plant for three days the author had a sufficient amount of data to analyze. The initial looks at the data while still in Arizona clearly showed the presence of SO_2. The absorption lines were distinct and obviously different from the Blue Sky background. This chapter presents the main results of this thesis, the remote measurement of atmospheric SO_2 with an imaging spectrometer.

B. RAW DATA

LINUS data is saved in a "flat format" data file. The camera output has a 12-bit dynamic range but data are saved as 16-bit integers. 12 bits can represent a number as large as $2^{12} = 4096$ which is the upper limit for the dynamic range of LINUS. Figure 23 depicts the hypercube which is the output of LINUS.

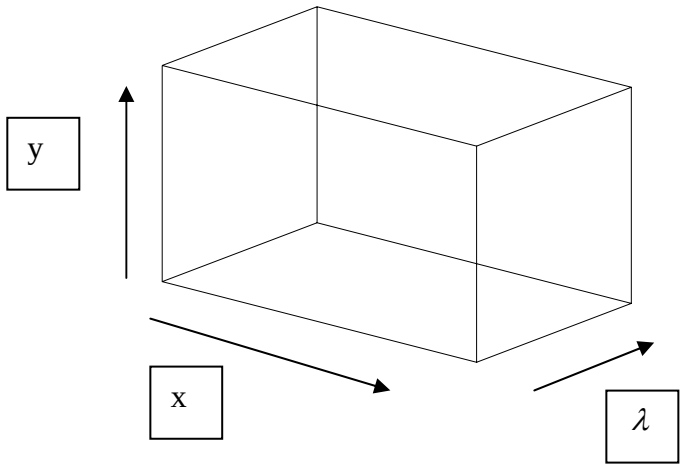

Figure 23 Hypercube image produced by LINUS

The y and λ dimensions are 512 each and the size of the x dimension is the number of horizontal steps (time sequence). Wavelengths range from 277.7 nm to 320 nm, with a resolution of 0.083 nm per column for the 0.1 mm slit width used at St. Johns.

To reduce the impact of the noise the data were averaged over the x and y directions. For much of the work the x direction was completely averaged out. After averaging across the x direction the hypercube collapses into a $512x512$ rectangular matrix as seen in Figure 24-basically a vertical profile.

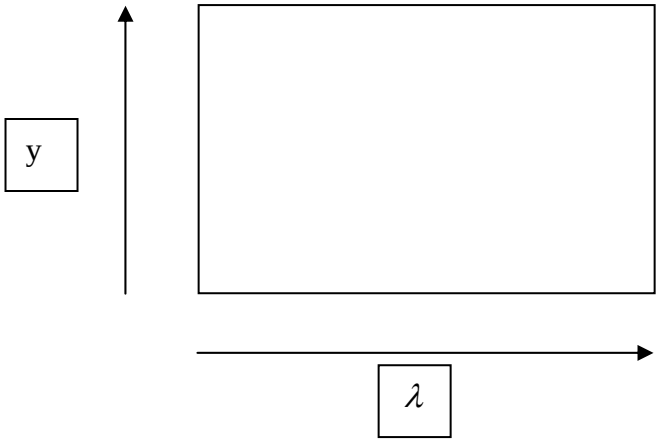

Figure 24 Hypercube after averaging the x-dimension ($512x512$ matrix)

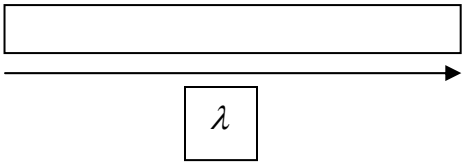

Figure 25 Hypercube after averaging over the x and y dimensions ($512x1$ matrix)

Averaging across the y dimension leaves a 512 x 1 vector L as seen in Figure 25.

C. FILTERING CONCEPT

SO_2 absorbs UV light at specific wavelengths. The basic idea of filtering is that any substance that attenuates sunlight can be considered as a filter. A conceptual approach using matrix algebra is used her to determine that filter effect.

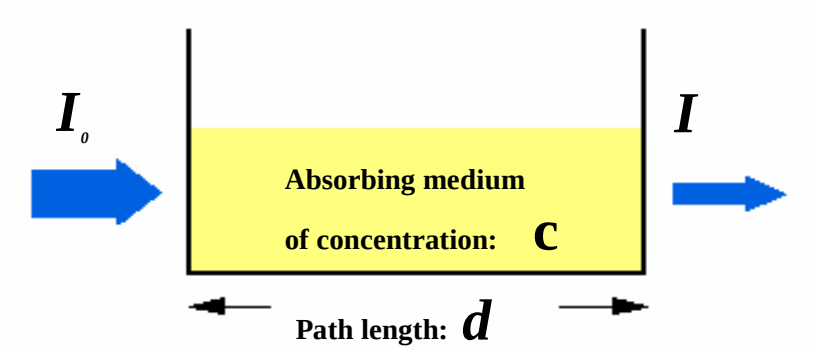

Figure 26 Filter Concept (from Marino)

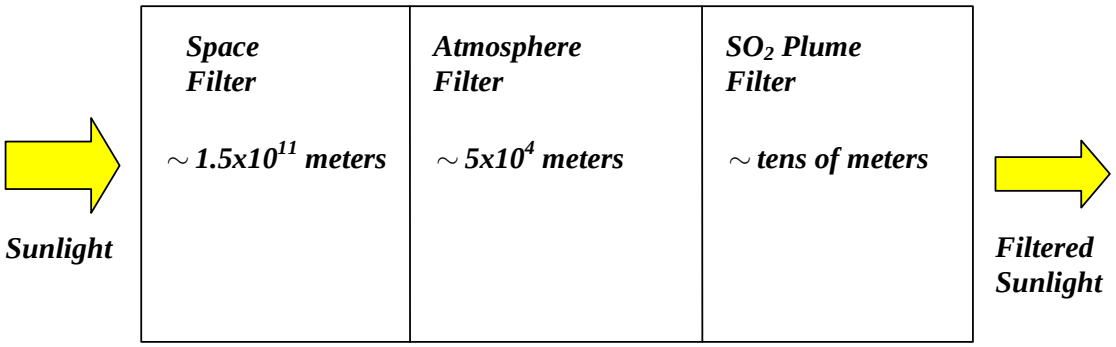

Figure 27 Space, Atmosphere, and SO_2 Plume filters

Figure 26 illustrates the filter concept. Light is emitted by the sun and its intensity is reduced on the way to earth by spherical spreading. There is also some absorption involved due to space dust but this is relatively minor. This can be considered as the "Space Filter". This light then enters the top of the atmosphere and is absorbed and scattered. This is the "Atmosphere Filter". Finally the light passes through an SO_2 plume and is further attenuated (as a function of wavelength). Since each filter is an attenuating filter, it is modeled as a 512 x 512 diagonal matrix with each diagonal entry less than or equal to 1.0. This idea is illustrated in Equations (3.3) and (3.4) and Figure 27. Since the filters are modeled as diagonal square matrices multiplication is commutative as well as associative.

In order to determine the Plume filter it is necessary to remove the effects of the Atmosphere. This is done using matrix algebra as seen in Equation (4.1).

$$PlumeFilter = Plume * Atmosphere^{-1} \tag{4.1}$$

$$Plume = \begin{bmatrix} p_{1,1} & 0 & \cdots & 0 \\ 0 & p_{2,2} & & 0 \\ \vdots & & \ddots & \vdots \\ 0 & 0 & \cdots & p_{512,512} \end{bmatrix} \tag{4.2}$$

$$Atmosphere = \begin{bmatrix} a_{1,1} & 0 & \cdots & 0 \\ 0 & a_{2,2} & & 0 \\ \vdots & & \ddots & \vdots \\ 0 & 0 & \cdots & a_{512,512} \end{bmatrix} \tag{4.3}$$

This then yields the Plume Filter. With this method of viewing the data the Blue Sky background has a transmission of one, and anything else that filters the sunlight will have a filter value between zero and one at any wavelength. It is important to remember to record an image of the Blue Sky background every 30 minutes or so. The intensity of UV varies significantly with sun angle.

This method then yields a Filter curve which is synonymous with a percent transmission curve. The x-axis is wavelength and the y-axis is percent transmission with all of the data being normalized so that Blue Sky has a transmission of 100%.

With the Plume Filter determined, the author was able to build upon the work completed previously by Marino and Khoo. Khoo had compiled data sets showing the effect of various SO_2 molecular abundances on the Plume Filter. These results are published in his thesis and some of his results are shown in Figure 28. The various curves show the percent transmission of UV light as it passes through SO_2 at various volume percents and pressures (where 1 Hg equals 1 Torr of pressure).

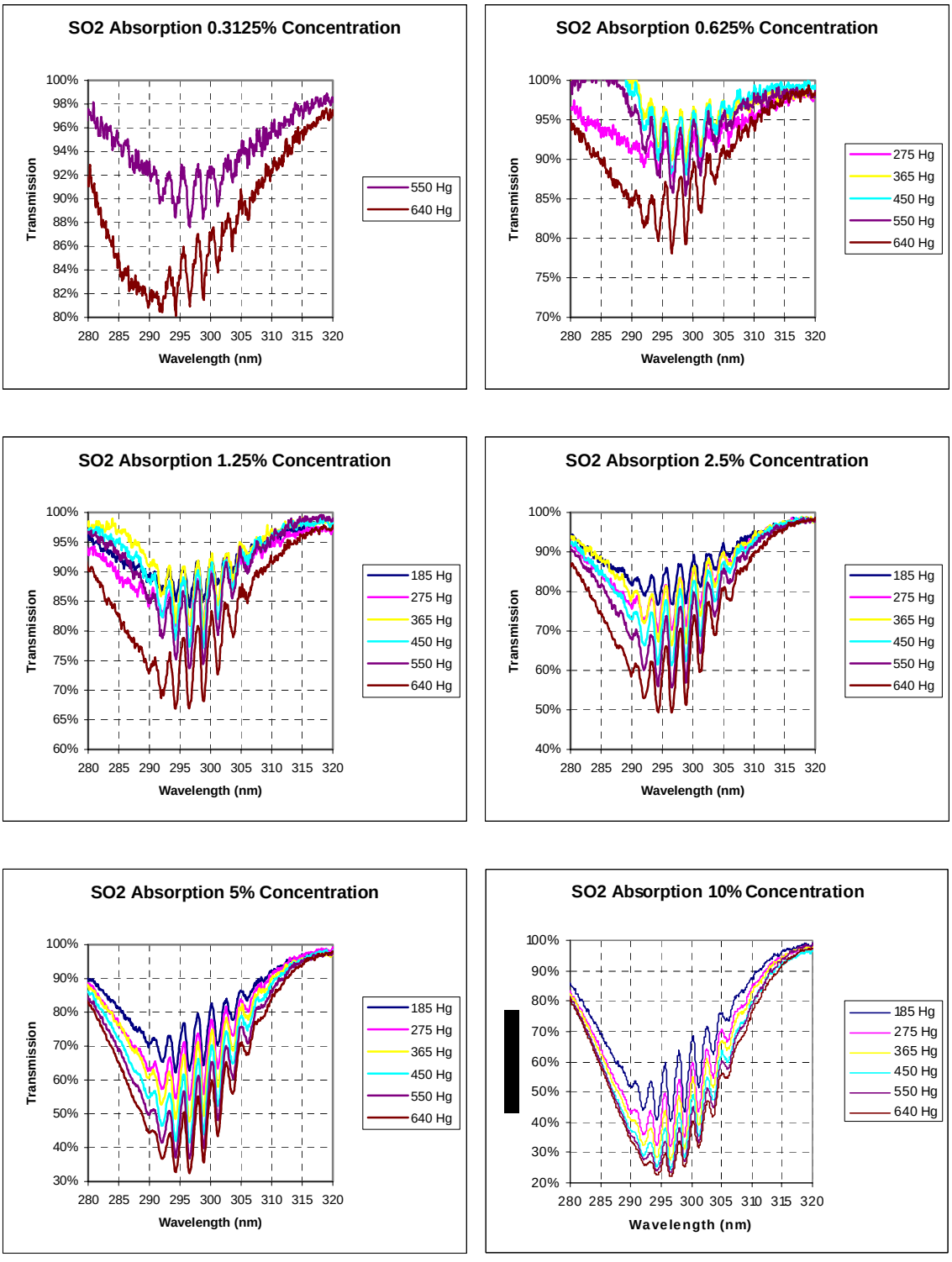

Figure 28 Lab data (Khoo, 2005)

D. CURVES OF GROWTH

The analysis technique used for this work makes use of curves of growth. Photons are absorbed by SO_2 as they pass through the plume. This absorption obeys the law:

$$-\delta I(\lambda) = I(\lambda)k(\lambda)dx \tag{4.4}$$

So $k(\lambda)$ is the fractional decrease in $I(\lambda)$ at wavelength λ per unit path length through the plume. The absorption coefficient $k(\lambda)$ is very important in determining the concentration of SO_2 in the plume. For a homogeneous plume of thickness ℓ Equation (4.4) can be integrated to yield

$$I(\lambda) = I_0(\lambda)e^{-k(\lambda)\ell} \tag{4.5}$$

This is for the simplified situation where there is one isolated absorption line. For multiple absorption lines

$$I(\lambda) = I_0(\lambda)e^{-\ell*\sum_{i=1}^{n}k_i(\lambda)} \tag{4.6}$$

$k(\lambda)$ has units of meter^{-1} and therefore $\ell * k(\lambda)$ is dimensionless as required. In order to determine the abundance of SO_2 in the plume it is necessary to find the area $\int_0^\infty k_i(\lambda)d\lambda$. This Area (referred to as Equivalent Width) is then plotted against the SO_2 column abundance to yield "Curves of Growth". Common practice is to plot the curves of growth on a log-log scale.

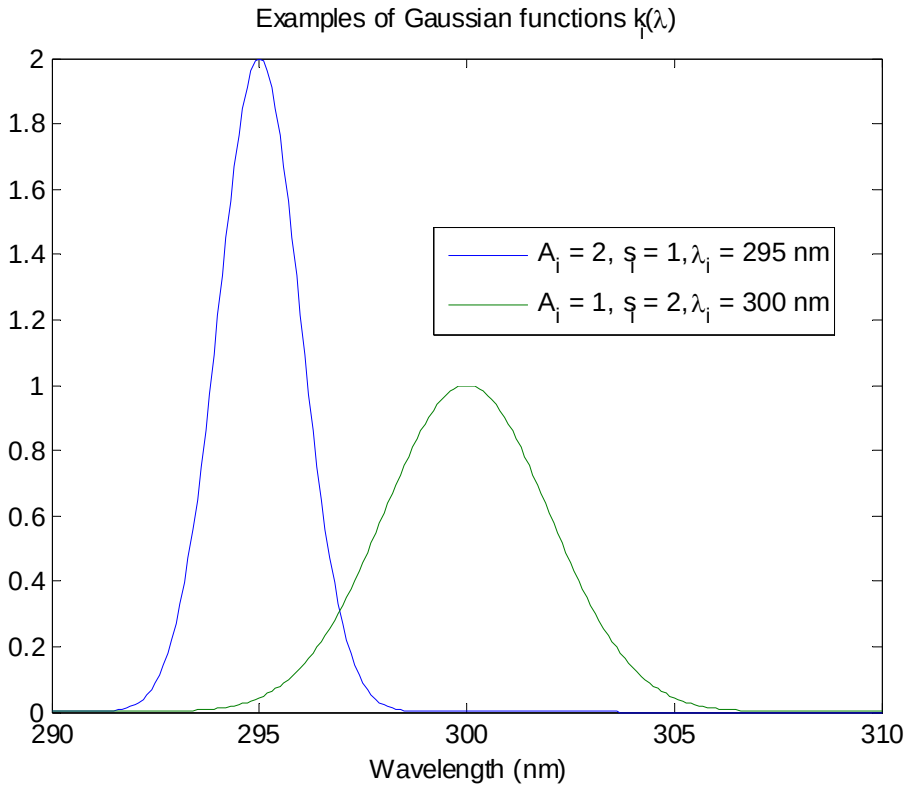

Figure 29 Examples of the Gaussian function $k_i(\lambda)$ (arbitrary units on vertical axis)

In order to determine $k(\lambda)$ for each absorption line a least squares fit of the data was conducted. Using Equation 3 we have

$$\ln(\frac{I(\lambda)}{I_0(\lambda)}) = -\ell\sum_{i=1}^{n} k_i(\lambda) \tag{4.7}$$

$I_0(\lambda)$ = 1 since we have normalized the data to the Blue Sky background. Therefore $\ln(I(\lambda)) = -\ell\sum_{i=1}^{n} k_i(\lambda)$ where each $k_i(\lambda)$ is modeled as a Gaussian, i.e.,

$$k_i(\lambda) = A_i e^{-(\frac{\lambda_i-\lambda}{s_i\sqrt{2}})^2} \tag{4.8}$$

It needs to be emphasized that the absorption coefficients are modeled as Gaussian, but this may not be their exact shape. The great advantage of using equivalent widths is that the analysis is fairly insensitive to whether a Gaussian or Lorentzian shape is assumed.[21]

[21] Thorne, et al.

Each $k_i(\lambda)$ therefore contains three unknown variables: amplitude (A_i), "standard deviation" (s_i), and wavelength (λ_i). λ_i is the central wavelength at which the maximum absorption due to $k_i(\lambda)$ occurs. The λ_i are known to some close approximation but allowing them to be considered as unknowns to some close approximation was found to be useful in fitting the data to a model. The data from Khoo showed seven distinct absorption lines with absorption peaks at about 292.2, 294.6, 296.8, 299.1, 301.4, 303.6, and 305.8 nm. The method used to solve for the 21 variables was to minimize z, the sum of the square of the errors.

$$z = \sum_{\lambda} (\ln(data) + \ell \sum_{i=1}^{n} k_i(\lambda))^2 \tag{4.9}$$

z is a function of A_1, …, A_7, s_1, …, s_7, λ_1, …, λ_7. From this $k_i(\lambda) = A_i e^{-(\frac{\lambda_i - \lambda}{s_i\sqrt{2}})^2}$ was derived. The integral in Equation (4.10)

$$\int_0^{\infty} k_i(\lambda) d\lambda = \frac{\sqrt{2\pi}}{2} A_i s_i (1 + \frac{2}{\sqrt{\pi}} \int_0^{\frac{\lambda_i}{s_i\sqrt{2}}} e^{-z^2} dz) \tag{4.10}$$

$$erf(\frac{\lambda_i}{s_i\sqrt{2}}) = \frac{2}{\sqrt{\pi}} \int_0^{\frac{\lambda_i}{s_i\sqrt{2}}} e^{-z^2} dz \tag{4.11}$$

was then calculated and plotted against column abundance. Equation (4.11) is the error function equation and is a standard function in most scientific software including MATLAB. The results are shown in Figure 30 and Table 2.

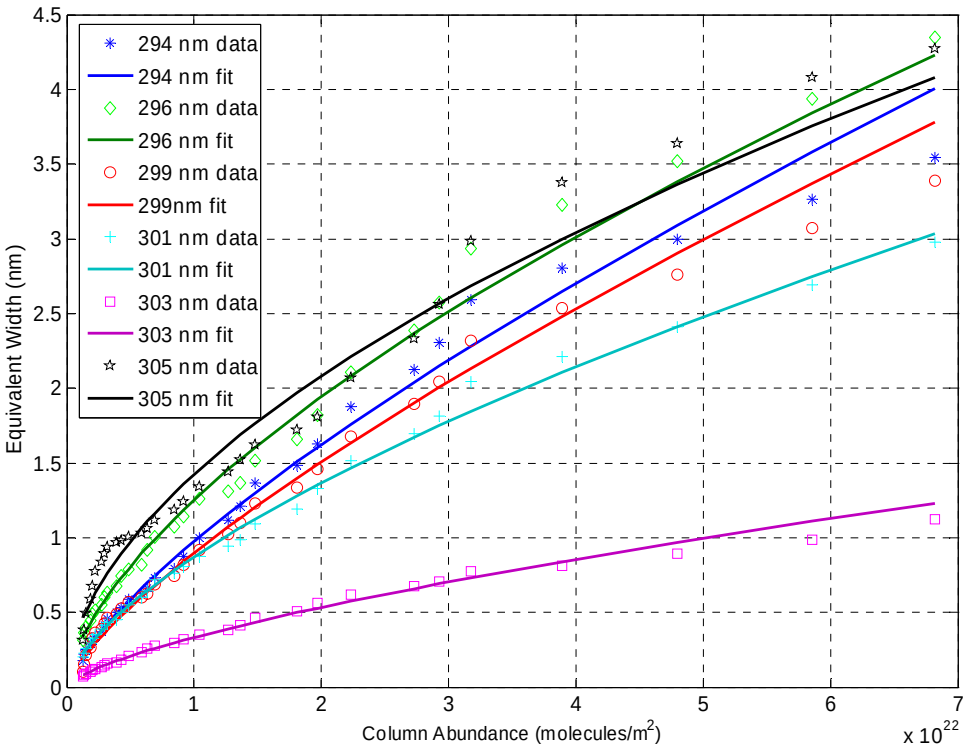

Figure 30 Equivalent Width versus Column Abundance

Wavelength(nm)		292.2	294.6	296.8	299.1	301.3	303.6	305.8
Column Abundance (molecules/m^2)	**1.28E+21**	0.0839	0.1770	0.3113	0.1023	0.2052	0.0719	0.3165
	1.38E+21	0.2837	0.2222	0.3499	0.1026	0.2323	0.0761	0.4012
	1.49E+21	0.3771	0.2710	0.4262	0.2464	0.2446	0.0968	0.4374
	1.83E+21	0.4220	0.2835	0.4506	0.3073	0.2791	0.0968	0.6156
	1.99E+21	0.5949	0.3205	0.4709	0.3087	0.3387	0.1145	0.7149
	2.26E+21	0.6067	0.3388	0.5296	0.3727	0.3818	0.1225	0.7635
	2.76E+21	0.6163	0.3388	0.5588	0.4106	0.3821	0.1378	0.8415
	2.96E+21	0.7828	0.4115	0.5589	0.4108	0.3893	0.1388	0.9269
	3.21E+21	0.8310	0.4498	0.6457	0.4453	0.4379	0.1597	0.9537
	3.93E+21	0.8431	0.5342	0.7023	0.5005	0.4640	0.1605	0.9854
	4.28E+21	0.8431	0.5477	0.7070	0.5470	0.4743	0.1877	0.9854
	4.84E+21	0.8635	0.5660	0.7745	0.5499	0.4788	0.1933	0.9924
	5.92E+21	1.0580	0.5699	0.8739	0.5719	0.6463	0.2290	0.9929
	6.35E+21	1.0964	0.7206	0.8750	0.6708	0.7008	0.2793	1.0823
	6.89E+21	1.0965	0.7207	0.8750	0.6708	0.7009	0.2793	1.0961
	8.43E+21	1.2152	0.7376	1.1951	0.6742	0.7030	0.2963	1.1544
	9.18E+21	1.4409	0.8960	1.1973	0.8525	0.8527	0.3125	1.2641
	1.04E+22	1.6001	0.9084	1.2183	0.8526	0.8624	0.3217	1.3362
	1.27E+22	1.6344	1.1077	1.2188	1.0302	0.9157	0.3834	1.3641
	1.36E+22	1.8110	1.3401	1.4601	1.1952	1.0392	0.4406	1.5756
	1.48E+22	1.8225	1.3417	1.4712	1.1997	1.0427	0.4415	1.6603
	1.81E+22	1.8292	1.3595	1.4717	1.2010	1.0626	0.4802	1.6639
	1.97E+22	2.4992	1.6971	1.9497	1.5351	1.4026	0.5823	1.8443
	2.23E+22	2.5032	1.6984	1.9505	1.5363	1.4047	0.5850	1.8483
	2.73E+22	2.9424	2.0470	2.2739	1.8307	1.7167	0.7164	2.0230
	2.93E+22	3.7759	2.5784	2.8848	2.2862	1.9777	0.7409	2.9618
	3.18E+22	3.7761	2.5974	2.8852	2.2866	1.9933	0.7510	2.9636
	3.89E+22	3.8219	2.5977	2.8860	2.2886	1.9939	0.7512	2.9969
	4.79E+22	5.2673	3.1288	3.7339	2.9151	2.5491	0.9138	3.9792
	5.86E+22	5.2685	3.1295	3.7341	2.9152	2.5494	0.9139	3.9793
	6.82E+22	6.1307	3.5423	4.3505	3.3908	2.9791	1.1261	4.2725

Table 2. Equivalent Width versus Column Abundance and Wavelength

Wavelength (nm)	Equation of Growth
292.2	$Width = -39.3985 + 0.7854\ln(ColumnAbundance)$
294.6	$Width = -37.2990 + 0.7358\ln(ColumnAbundance)$
296.8	$Width = -31.9166 + 0.6345\ln(ColumnAbundance)$
299.1	$Width = -38.0704 + 0.7494\ln(ColumnAbundance)$
301.3	$Width = -33.1185 + 0.6510\ln(ColumnAbundance)$
303.6	$Width = -35.6703 + 0.6824\ln(ColumnAbundance)$
305.8	$Width = -27.4336 + 0.5485\ln(ColumnAbundance)$

Table 3. Equations relating Equivalent Width to Column Abundance

Using the data shown in these tables it is possible to fit a logarithmic curve to the data.

$$\begin{bmatrix} \ln(y_1) \\ \ln(y_2) \\ \vdots \\ \ln(y_n) \end{bmatrix} = \begin{bmatrix} a \\ a \\ \vdots \\ a \end{bmatrix} + \begin{bmatrix} b\ln(x_1) \\ b\ln(x_2) \\ \vdots \\ b\ln(x_n) \end{bmatrix} \tag{4.12}$$

So,

$$\overline{\ln(y)} = \begin{pmatrix} 1 & \ln(x_1) \\ 1 & \ln(x_2) \\ \vdots & \vdots \\ 1 & \ln(x_n) \end{pmatrix} \begin{bmatrix} a \\ b \end{bmatrix} \tag{4.13}$$

This equation is of the form $\bar{y} = \bar{\bar{x}}\bar{z}$ where $\bar{z} = \begin{bmatrix} a \\ b \end{bmatrix}$. So, $\bar{z} = (\bar{\bar{x}}^T \bar{\bar{x}})^{-1}(\bar{\bar{x}}^T \bar{y})$.

Using this least squares fit the Equations of Growth for each specific absorption wavelength were calculated and are shown in Table 3 and plotted in Figure 30.

E. QUANTIFICATION

In the field a test cell containing a known amount of SO_2 is imaged at least once each day. This provides assurance that LINUS is still working properly and is a second check to the curves of growth. The test cell was placed in front of the aperture as seen in Figure 31. The raw test cell data is not a pure SO_2 signature; it also necessarily contains

the atmospheric spectra and any interference from the test cell itself. Both of these contributions were divided out to yield a pure SO_2 spectrum.

Figure 31 Author holding test cell in front of LINUS aperture

In order to quantify the amount of SO_2 being seen it is necessary to have a reference. Khoo's lab work and the author's subsequent analysis of that work provided the reference Curves of Growth shown in Figure 30.

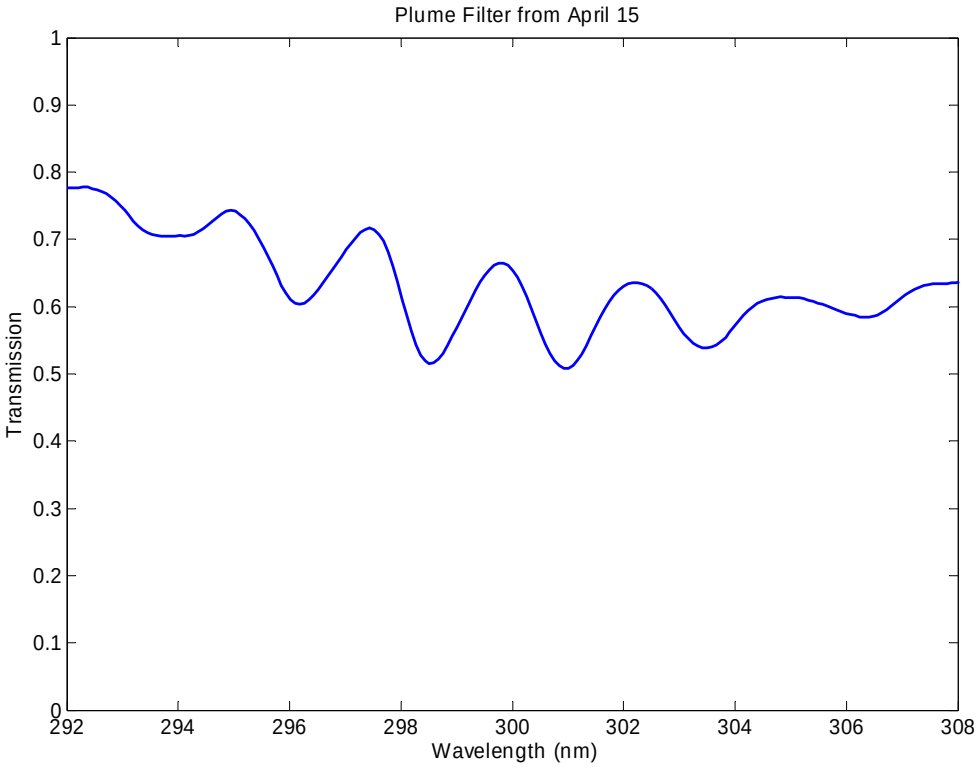

Figure 32 Plume data from April 15 Right Stack

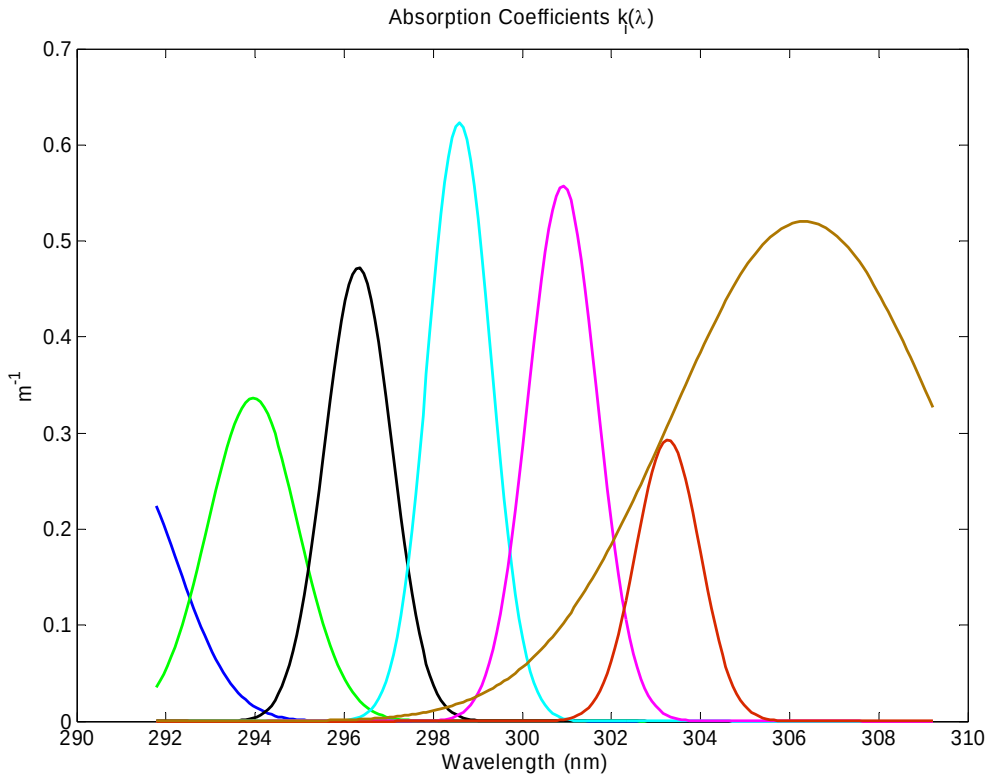

Figure 33 Absorption coefficients $k_i(\lambda)$ for the April 15 Right Stack Plume Filter

All of this work then provides the basis to analyze data taken in the field. The field data were analyzed in the same way that Khoo's data were analyzed. The field data were fit to the model $I(\lambda) = I_0(\lambda)e^{-\ell^* \sum_{i=1}^{n} k_i(\lambda)}$ where each $k_i(\lambda) = A_i e^{-(\frac{\lambda_i - \lambda}{s_i \sqrt{2}})^2}$. Then the equivalent width (integral) of each $k_i(\lambda)$ was calculated, $\int_0^\infty k_i(\lambda) d\lambda$. These equivalent widths were then compared to the equations of growth shown in Table 3.

As seen in Figure 33 the absorption coefficient functions overlap. It is desirable to use the $k_i(\lambda)$ nearest the center of the wavelength band due to less interference from the less accurate $k_i(\lambda)$ at the edges of the band. It is important to minimize error in the equivalent width measurements because there is an exponential relationship between the equivalent width and column abundance.

In order to more easily compare data between LINUS and the actual power plant SO_2 emissions reported by SRP it was convenient to talk in terms of "ppm-m" instead of "column abundance". This is because power plant emissions are commonly reported in ppm. A ppm-m is used to describe a photon traversing a distance of 1 meter through an SO_2 plume which has a concentration of 1ppm. As an example, suppose a plume of thickness 2 m has an SO_2 concentration of 200ppm. This plume would then be reported as having an abundance of 400ppm-m (assuming 100% measuring accuracy). The

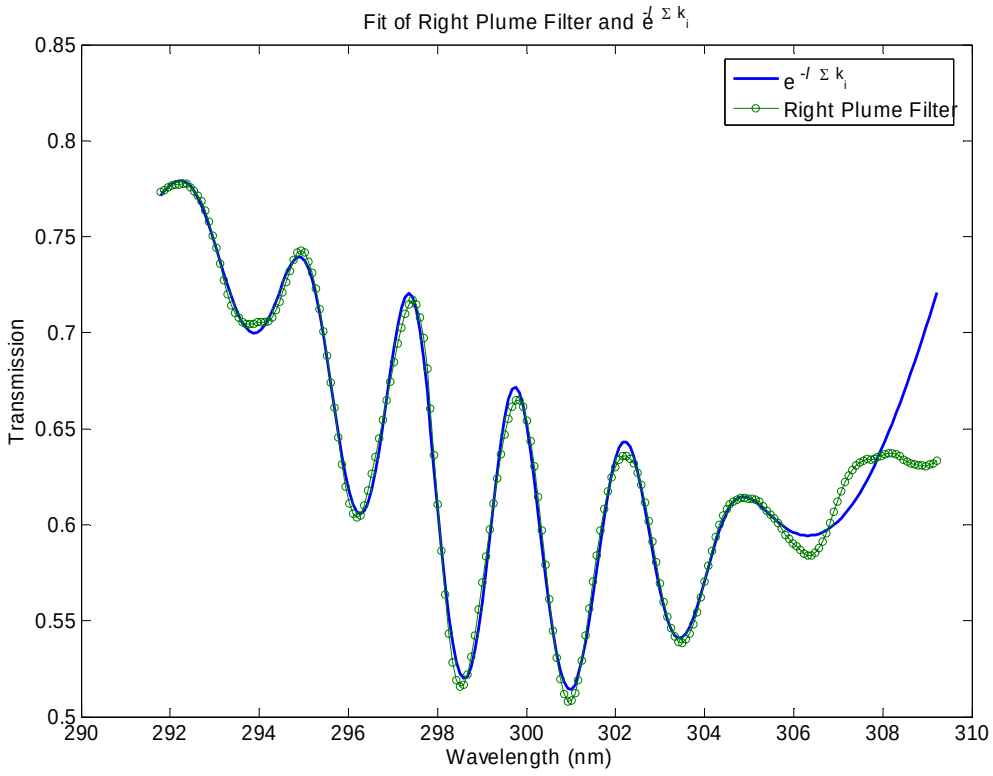

Figure 34 Fit between 15 April Right Stack Plume Filter and the fitted curve

exhaust stacks for the SRP Coronado plant have a diameter of 5.7 m at the top. Therefore, for a first order estimate of the concentration of SO_2 in the exhaust the following procedure was used:

1) Determine the equivalent width of the data at a given wavelength

2) Convert equivalent width to ppm-m

3) Divide this number by 5.7 m

This gives the concentration of the exhaust in ppm. As an example, the equivalent width at $\lambda_i = 296nm$ for the Right Stack Plume data taken on 15 April is 2.05 nm. Using Figure 30 this equates to about 2.3x10^{22} molecules/m^2 which equates to 900 ppm-m SO_2. $\frac{900\,ppm-m}{5.7m} = 158\,ppm$. The actual stack output provided by SRP at 0930 was 203.5 ppm. Using the equivalent width of 1.6 nm at $\lambda_i = 299nm$ yields about 175 ppm. An

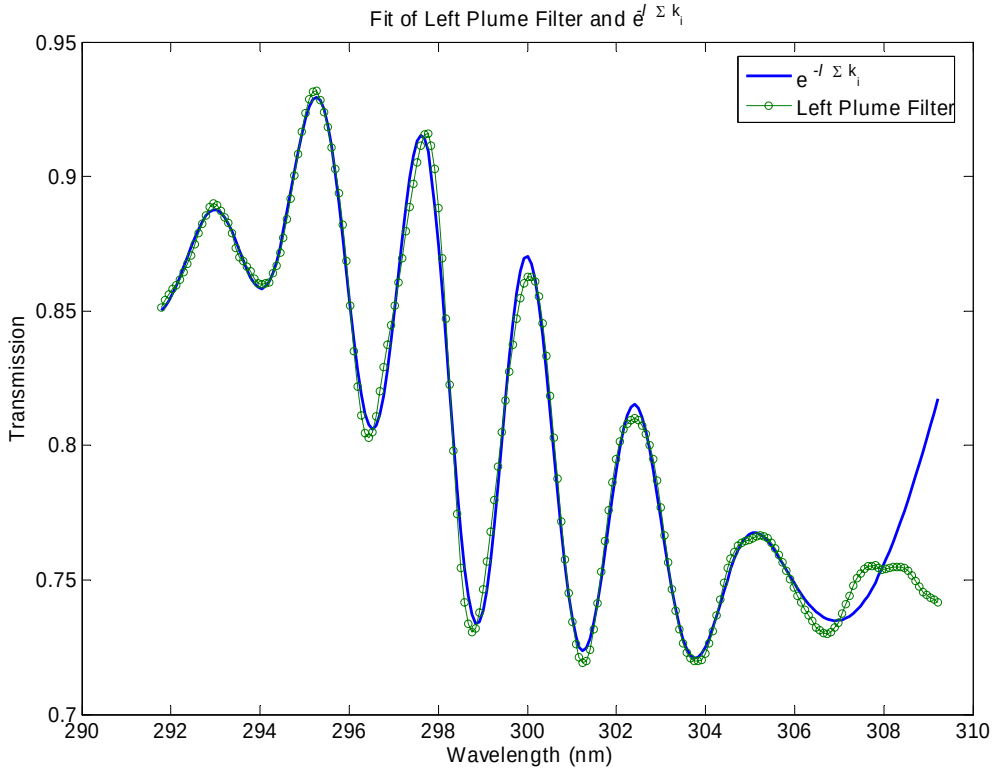

Figure 35 Fit between 15 April Left Stack Plume Filter and the fitted curve

image taken ten minutes later of the left stack had an equivalent width of 1.35 nm at $\lambda_i = 296nm$. Using the equation from Table 3 this equates to 1.2x10^{22} molecules/m^2 which equates to 500 ppm-m SO_2. $\frac{500\,ppm-m}{5.7m} = 88\,ppm$. The actual stack output provided by SRP at 0930 was 86 ppm. The equivalent width of 0.99 nm at $\lambda_i = 296nm$ gives the same answer.

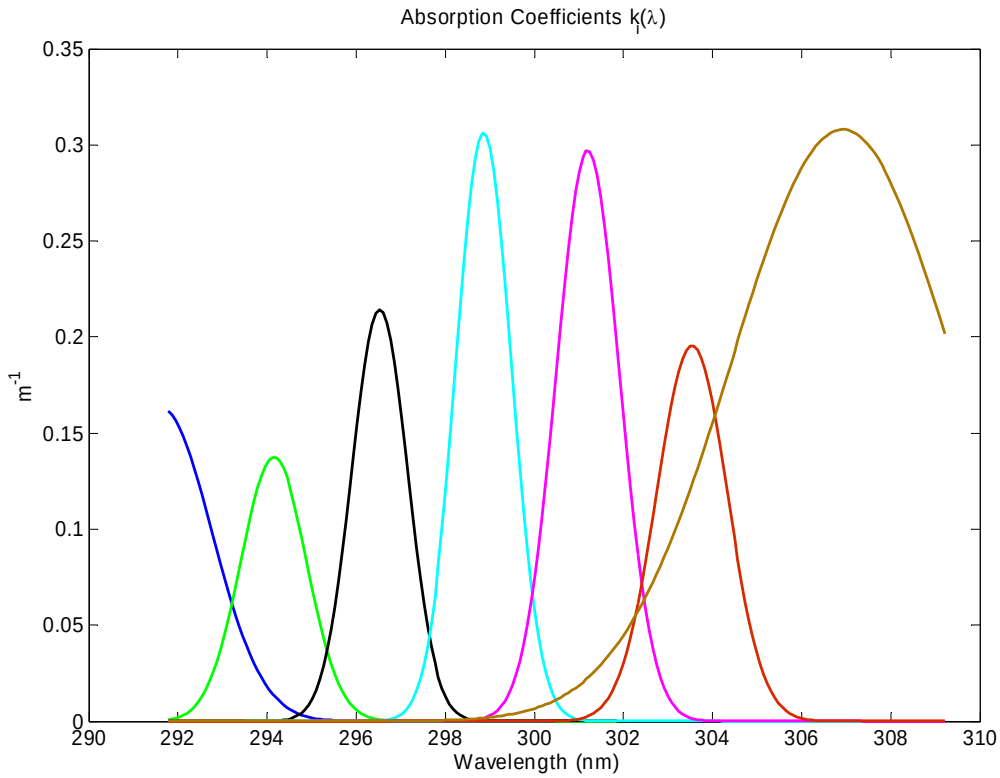

Figure 36 Absorption coefficients $k_i(\lambda)$ for the April 15 Left Stack Plume Filter

Figure 37 and Table 4 provide a summary of SO_2 concentrations determined from various images. The ppm calculated from the equivalent width of the 296 nm and 299 nm absorption coefficients are presented. As mentioned previously these are the absorption coefficients which have the least overlap with coefficients on the edge of the wavelength band and are therefore considered most accurate.

The two data from Set 1 are coincident. The data from Set 6 are very nearly equal to the output of the left stack. The rest of the data falls between the left and right stack ppm with the exception of Data Set 3. There could be various reasons for these differences such as wind speed and direction and the magnitude of time between taking the Blue Sky background scene and imaging the plume. The main reason that some results are low is due to averaging across blue sky and structure instead of plume. Recommendations are made in Chapter V to reduce these variances.

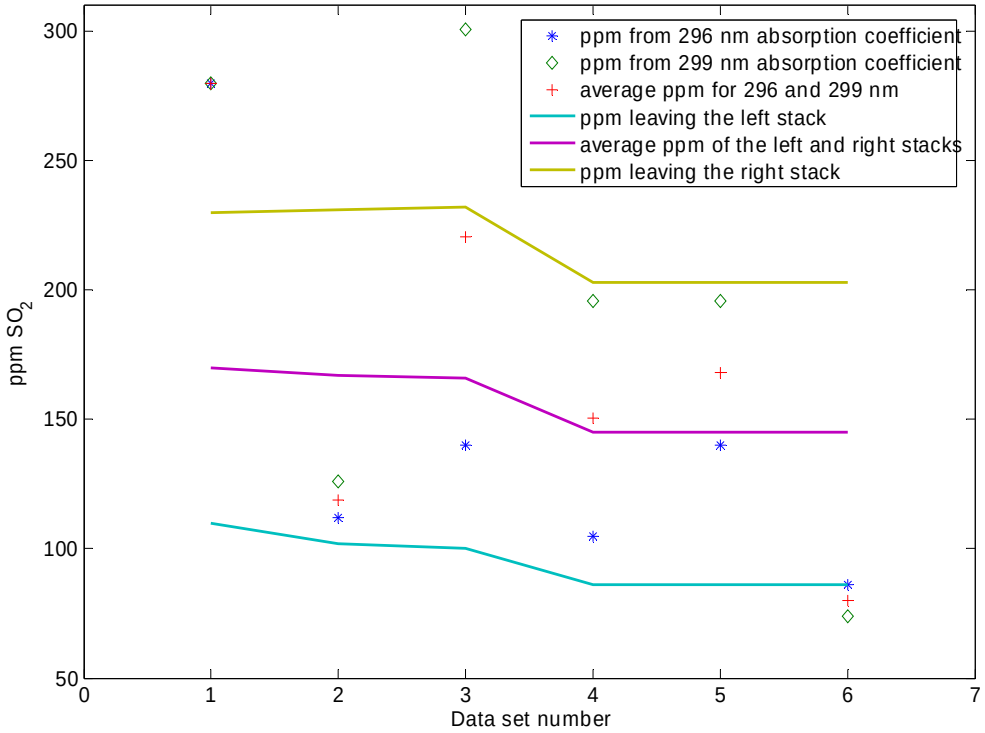

Figure 37 Summary of six different images of the smoke stacks

Data Set number	Description
1	Right plume
2	Center plume
3	Center plume
4	Center plume
5	Right plume
6	Left plume

Table 4. Description of data sets

F. SPECTRAL IMAGING

Quantitative analysis, as given above, required averaging out the horizontal spatial information. Still, LINUS is an imaging system and does provide the opportunity to test standard spectral imaging techniques.

Figure 38 shows the results of two classification efforts for the full spectral cube. On the left is the result of an analysis using the spectral angle mapper algorithm. This classification approach was done by taking representative regions of interest for the blue

sky and plume, then running the classifier with the resulting exemplar spectra. The resulting classification effort is encoded with blue for sky, red for the plume (SO_2).

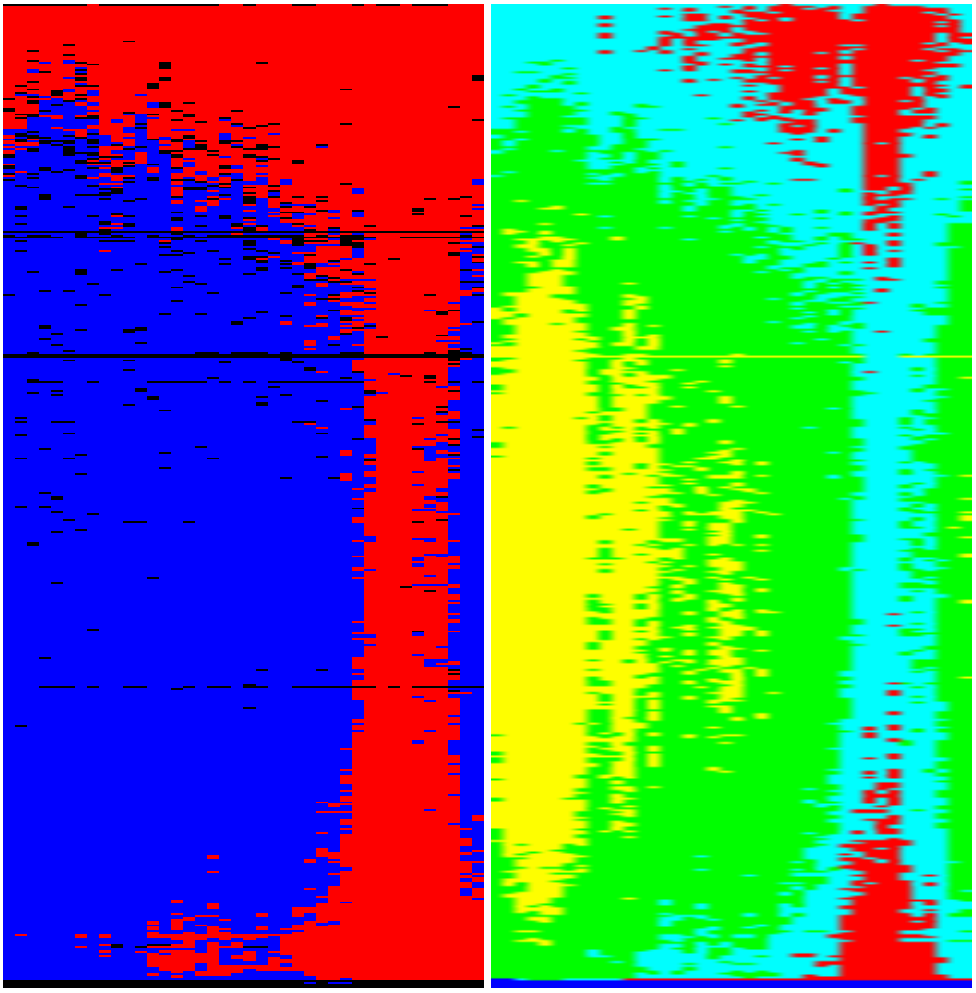

Figure 38 Classification images of the left stack (each image 19 m wide by 5 m high)

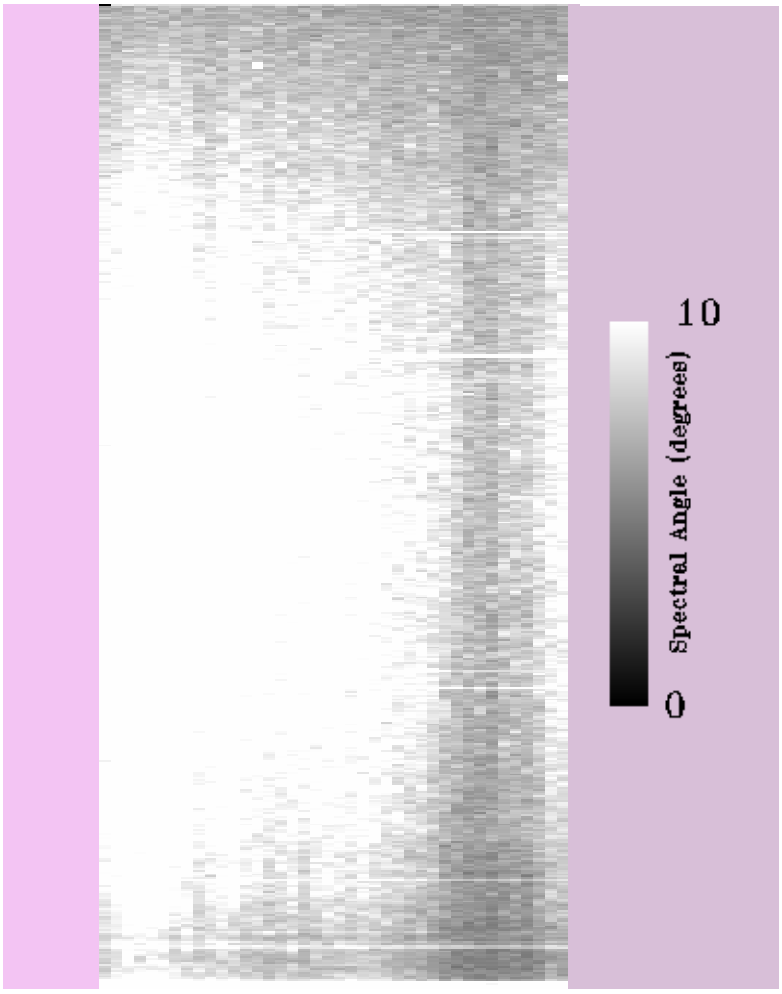

Figure 39 Rule image for the Plume spectra

Figure 39 shows the measure for the difference between the plume exemplar and the point-by-point spectral data. The plume proper gives an angle of 5 degrees or so between the examplar and plume. On the right side of Figure 38, the results of an ISODATA analysis are shown. Four classes were selected, and the algorithm clearly was able to distinguish between sky and plume, although the classes apparently show an effect due to overall illumination (brightness) with altitude.

The author also wrote a MATLAB program to analyze each scene in an image and output the average ppm SO_2 in each scene based upon a 5.7 meter diameter plume. This output for the left plume is shown in Figure 40 and agrees favorably with the ENVI classification images. The entire image seen in Figure 38 and Figure 40 is 19 meters

across by 5 meters high and the left stack is seen in the right third of the image. Figure 41 displays the Plume Filter for each of the 40 scenes in this same image. It should be noted that some of the values are greater than one, which shouldn't happen if the plume is normalized to the background. This is an artifact of the difference in background sky brightness due to the time difference between the Blue Sky image and the Plume image. There is also an effect from the sun angle difference since LINUS necessarily points away from the plume to get a Blue Sky image. Recommendations to minimize these effects are covered in Chapter V.

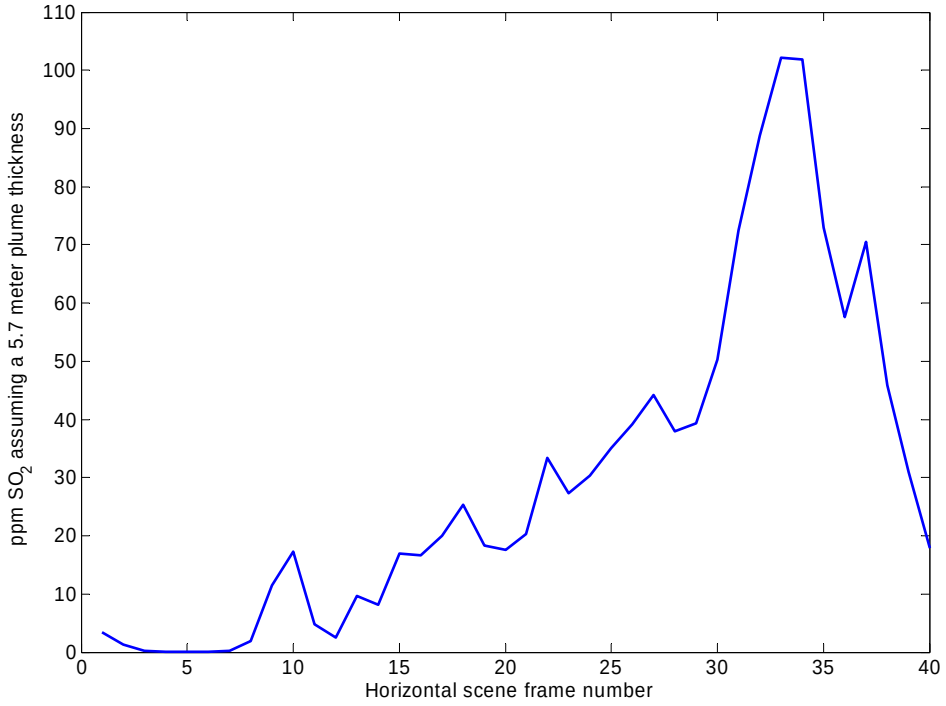

Figure 40 ppm SO_2 assuming a 5.7 meter diameter plume

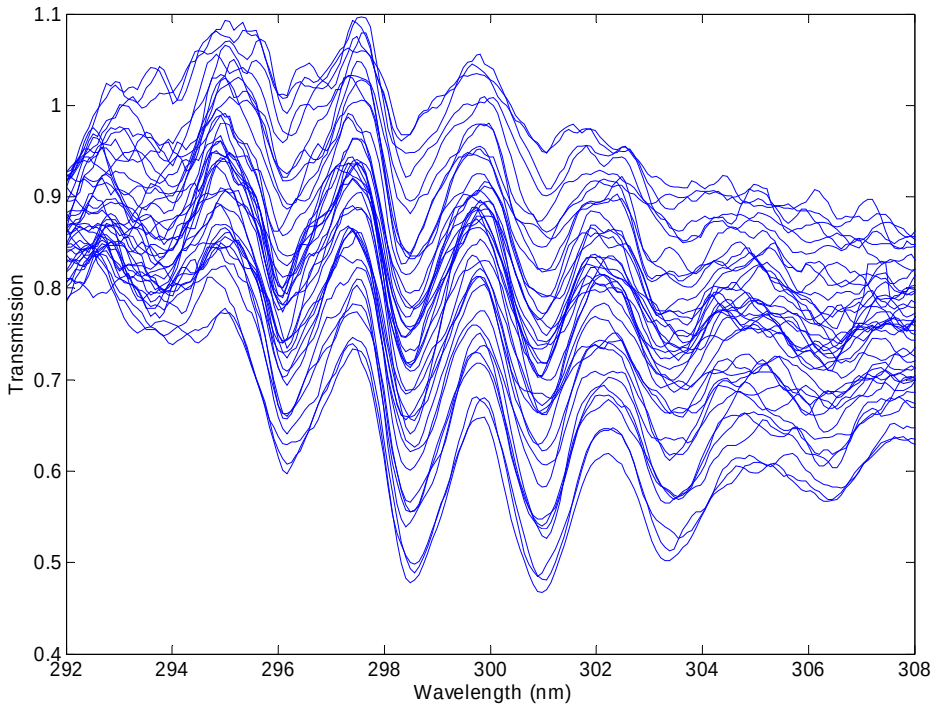

Figure 41 Variation in plume transmission across 40 scenes

V. CONSIDERATIONS FOR FOLLOW-ON ACTIVITIES

A. SALT RIVER PROJECT CORONADO PLANT

Another trip to the SRP Coronado power plant is recommended. This trip should focus on imaging the stacks from various distances in order to determine the maximum distance at which LINUS can detect and quantify SO_2. It would be useful to attempt to image even up to 8 kilometers distant. It would also be useful to image the stacks from various angles as depicted in Figure 42 and Figure 43. This would provide the benefit of imaging greatly varying concentrations, particularly if the concentrations from stacks 1 and 2 vary significantly. While taking field data particular attention should be paid to the width of scene that is being imaged. A laser range finder should be purchased to assist in field work.

B. POST REFURBISHMENT CAMERA CALIBRATION

Prior to another data gathering trip the Princeton camera is being refurbished and another lab calibration of LINUS will need to be completed. This calibration will verify the wavelength calibration and provide new curves of growth. This is needed because the camera characteristics may have changed while being refurbished.

A new test cell filling apparatus needs to be constructed, including a new more accurate pressure gauge. In addition, a new test cell has been acquired.

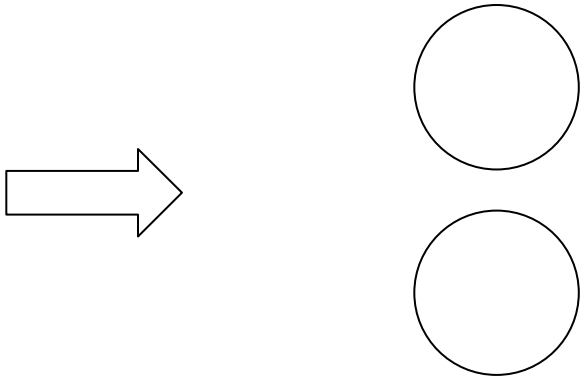

Figure 42 Broadside view showing smoke stacks and viewing direction

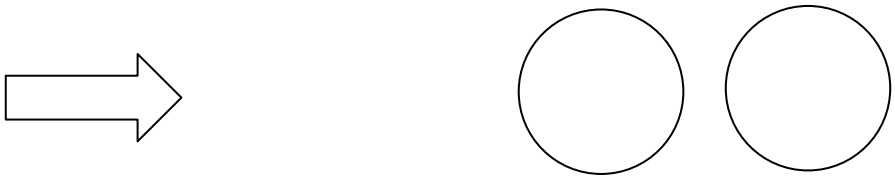

Figure 43 End-on view showing smoke stacks and viewing direction

C. MOUNT SAINT HELENS

Following another trip to SRP Coronado it is recommended that a trip to Mount St. Helens be undertaken. The author traveled to Mount St. Helens in December 2004 to scout out the area. The earliest possible time to go is mid-June with July being more likely. Some of the roads do not open until July due to snow. Two locations in particular are recommended as observation spots, Johnston Ridge Observatory and Lahar. The nearest that any public access paved road approaches the crater is at a distance of about 7 km. Lahar which is on Road 83 is just about 7 km southeast of the crater. Johnston Ridge Observatory is located about 8 km almost due north of the crater.

D. GENERAL RECOMMENDATIONS

It is recommended that a standard file naming system be employed. The following system was used and was useful: Date_SceneDescription_Exposure_MCPvoltage_slitwidth_NumberofHorizontalSteps. For example, April15_leftstack_13_850_1_10.dat is an image taken on April 15 of the left smoke stack, 13 second exposure per step, MCP voltage 850 volts, 0.1 mm slit width, and 10 horizontal steps. When the file is saved the computer will give it a timestamp in case the exact time is needed. This is how the comparisons were made with the SO_2 data provided by SRP. Care must be taken to record exactly the location the camera was pointed in order to use corroborating data. This could have been done better on the St. Johns trip, but where this information was known the error bound was within about 20%.

The existing LINUS UV filter is not optimal for SO_2. It would be very beneficial for LINUS to be modified to accept various UV filters. This might be done with removable filters or perhaps a rotary type disc containing various filters. A wavelength calibration would need to be performed for each filter. This would allow imaging over a wider range of wavelengths and should even facilitate attempts to detect molecules other than SO_2.

Since sun angle has a great effect on the amount of UV reaching the camera, it is recommended that a Blue Sky background scene be taken within 30 minutes of any image. The Blue Sky background should also be taken with LINUS pointing as close to the same general direction as the Plume as possible without including SO_2 in the background.

Care must be taken to take long enough exposures to take full advantage of LINUS's dynamic range. Making full use of the dynamic range will raise the signal-to-noise ratio (SNR) and greatly aid in extracting useful data. Figure 12 illustrates the filter response function and transmission drops off rapidly below 290 nm and above 310 nm.

Exhaust from the stacks contains some water vapor and other chemicals. It would be instructive to account for these effects (if any), possibly using MODTRAN.

THIS PAGE INTENTIONALLY LEFT BLANK

VI. SUMMARY

The trip to Arizona was a success. The presence of SO_2 was easily determined and quantification to within about 20% was accomplished (when target area was clearly identified). This work differed from previous LINUS work in that the processes and procedures to quantify what is seen in the field are now well known. Procedures have been written and code developed to allow this analysis to occur in the field immediately after collecting data. This will allow corrections to methods to be made on the spot if required.

LINUS has been proven to be a capable instrument and now needs to be used in various scenarios as recommended in Chapter V.

Possible uses for this technology include remote verification of industry emissions, reporting detection of unreported SO_2 sources, and possibly even inference of processes occurring in areas which are inaccessible. There may even be uses for LINUS using artificial illumination.

Hurdles still exist. Modifying LINUS to accept various filters and miniaturizing the technology are needed. It is easy to imagine this technology in an easy to carry size and the possibilities that would present. Accuracy would be improved by viewing a wider bandwidth. Then the data could be fit using a larger number of absorption lines and the absorption coefficients near the center of the band would be more accurate.

LINUS needs to be able to detect various gases, perhaps simultaneously. I see little to no difficulty in extending the present methods as long as the resolution is fine enough to separate out the absorption peaks of the different gases.

THIS PAGE INTENTIONALLY LEFT BLANK

APPENDIX. LINUS FIELD CHECKLIST

Initials	Item to Check
_____	LINUS: All accesses closed on case and all parts securely fastened down
_____	Generator: Check gasoline and oil levels, Test to ensure it runs
_____	Gasoline and oil(10W-30) for generator: Load extra cans (if required)
_____	Extension cords: Load sufficient number. Number loaded _____
_____	Power Strip: Loaded in truck
_____	Packing/Damping materials: Loaded in truck (if required)
_____	Permits: Loaded in truck (if required)
_____	GPS unit: Loaded in truck
_____	Extra batteries
_____	Multimeter
_____	Weather meter
_____	Screwdriver, toolbox
_____	Tape
_____	Sun shielding cardboard box
_____	Cell phone, leave number in office
_____	White sheets of sun protection
_____	Black felt for light pollution control

Day of Departure

_____	LINUS: Loaded in truck
_____	Base for LINUS: As required
_____	SO_2 calibration source: Loaded in truck
_____	Normal digital camera: Loaded in truck. Ensure sufficient memory
_____	Lint-free cloth: Loaded in truck

THIS PAGE INTENTIONALLY LEFT BLANK

LIST OF REFERENCES

Brassington, D. J., "Sulfur Dioxide Absorption Cross-Section Measurements from 290 nm to 317 nm," Journal of Applied Optics, v. 20, pp. 3774-3779, 1981.

Cabezas, R, "Design of a Bore Sight Camera for the Lineate Image Near Ultraviolet Spectrometer (LINUS)," Master's Thesis, Naval Postgraduate School, Monterey, California, June 2004.

Davis, S.C., Harkins, R.M., Olsen, R.C., "The LINUS UV Imaging Spectrometer," Proceedings of SPIE 5093, pp. 748-757, 2003.

Durkee, P.A., "MR 3480 – Thermodynamic and Radiative Processes in the Atmosphere," http://www.met.nps.navy.mil/~durkee/MR3480/MR3480.htm, November 18, 2005.

Finlayson-Pitts, B.J., Pitts, J.N. Jr., *Atmospheric Chemistry: Fundamentals and Experimental Techniques*, John Wiley and Sons, New York, New York, 1986.

Gray, J, "Design and First Operations of the Lineate Image Near Ultraviolet Spectrometer (LINUS)." Master's Thesis, Naval Postgraduate School, Monterey, California, December 2002.

Halvatzis, A.G., "Passive Detection of Gases In The Atmosphere. Case Study: Remote Sensing of SO_2 In the UV Using LINUS," Master's Thesis, Naval Postgraduate School, Monterey, California, December 2002.

Khoo, S.S., **"**Remote Sensing of Sulfur Dioxide (SO_2) using the Lineate imaging near-UltraViolet spectrometer (LINUS)," Master's Thesis, Naval Postgraduate School, Monterey, California, March 2005.

Kompatzki, R.C., "Design and Development Of The Image Scanner For Lineate Imaging Near Ultraviolet Spectrometer (LINUS)," Master's Thesis, Naval Postgraduate School, Monterey, California, December 2000.

Mares, A. G., "Remotely Sensed Density Measurements of Volcanic Sulfur Dioxide Plumes Using a Spectral Long Range Infrared Imager", Master's Thesis, Naval Postgraduate School, Monterey, California, September 2002.

Marino, S.A., "Operation and Calibration of the NPS Ultraviolet Imaging Spectrometer (NUVIS) in the Detection of Sulfur Dioxide Plumes," Master's Thesis, Naval Postgraduate School, Monterey, California, December 1999.

McGonigle, A. J. S., Hilton, D. R., Fischer, T. P., Oppenheimer, C., "Plume velocity determination for volcanic SO_2 flux measurements", Geophysical Research Letters, Volume 32, Number 11, American Geophysical Union, June 2005.

Southern Technologies, Inc., Longwood, Florida, http://www.southerntechnologies.com, October 1, 2005.

State of Arizona Official Website, http://az.gov, November 10, 2005.

Thorne, A., Litzen, U., and Johansson, S., *Spectrophysics: Principles and Applications*, Springer-Verlay, Berlin, Germany, 1999.

United States Environmental Protection Agency, http://www.epa.gov, October 3, 2005.

United States Geological Survey (USGS), http://vulcan.wr.usgs.gov/Volcanoes/MSH/framework.html, October 3, 2005.

INITIAL DISTRIBUTION LIST

1. Defense Technical Information Center
   Ft. Belvoir, Virginia

2. Dudley Knox Library
   Naval Postgraduate School
   Monterey, California

3. Richard C. Olsen, Code PH OS
   Naval Postgraduate School
   Monterey, California

4. Christopher Brophy, Code MAE BR
   Naval Postgraduate School
   Monterey, California

5. Richard Harkins, Code PH HK
   Naval Postgraduate School
   Monterey, California

6. Angela Puetz, Code PH
   Naval Postgraduate School
   Monterey, California